ANL/ACEA
103

ANL/ACEA
103

AN INTRODUCTION TO Ge(Li) AND NaI GAMMA-RAY DETECTORS FOR SAFEGUARDS APPLICATIONS

by

L. A. Kull

ARGONNE CENTER FOR EDUCATIONAL AFFAIRS

ACEA

DISCLAIMER

ARGONNE CENTER FOR EDUCATIONAL AFFAIRS

ACEA PROGRAMS • • •

- **Faculty**
  - Faculty Research Participation
  - Faculty Workshops
  - Conferences
  - Short Courses
- **Graduate**
  - Pre-doctoral Thesis
  - Thesis Assistance (short-term)
  - Conferences
  - Summer Engineering Practice School
  - Summer Biology Research Institute
  - Summer Materials Science Institute
  - Reactor Experiments
  - Argonne Semester in Science Communication
- **Undergraduate**
  - In-term Honors Research
  - Summer Student Research Training
  - Student-faculty Science Experiments
- **General**
  - Nuclear Materials Safeguards Training
  - Special Training Courses
  - Conferences

Argonne National Laboratory

For Further Information write to:
Argonne Center for Educational Affairs
9700 South Cass Avenue
Argonne, Illinois 60439

ANL/ACEA-103

ARGONNE NATIONAL LABORATORY
9700 South Cass Avenue
Argonne, Illinois 60439

AN INTRODUCTION TO Ge(Li) AND NaI GAMMA-RAY DETECTORS FOR SAFEGUARDS APPLICATIONS

by

L. A. Kull*

Consultant to

Safeguards Technical Services Organization
Brookhaven National Laboratory

and

Safeguards Training School
Argonne National Laboratory

Written June 1971
Revised February 1973
Published September 1974

JRB-71-105-I.J

* JRB Associates, Incorporated, P. O. Box 1393, 1250 Prospect Street, La Jolla, Calif. 92037. 714/459-2601

TABLE OF CONTENTS

LIST OF FIGURES

LIST OF FIGURES (Con't)

LIST OF FIGURES (Con't)

LIST OF TABLES

1. INTRODUCTION

Gamma-Rays From Special Nuclear Materials

All samples of nuclear material commonly found in the nuclear fuel cycle emit measurable amounts of natural radioactivity. The emitted radiation consists of neutrons, alpha-, beta-, and gamma-rays. These radiations are produced when the heavy elements such as uranium, plutonium, and thorium undergo natural nuclear transformations into different elements. Elements which undergo these natural transformations are called "unstable" and a parameter used to characterize their instability is the half-life.

The half-life of an unstable element is the time required for half of the original atoms to disintegrate by emitting radiation, and thus be transformed into a different element. For example, after 710 million years half the atoms in an intially pure sample of ^{235}U (uranium) will have disintegrated, emitting alpha and gamma-rays, to become atoms of ^{231}Th (thorium). The ^{231}Th atoms are also unstable and transform into ^{231}Pa (protactinium) emitting beta and gamma-rays. This process has a half-life of 25.6 hours. The unstable ^{231}Pa disintegrates into another unstable atom and the process of successive disintegration continues until ^{207}Tl (thallium) disintegrates into the stable nucleus, ^{207}Pb (lead). This particular "chain" of naturally radioactive elements is

known as the actinium series and is illustrated in Fig. 1.1 and listed in Table 1.1. A detailed energy level diagram for the first step in the chain is shown in Fig. 1.2, illustrating the origin of gamma rays from excited states of ^{231}Th following the alpha decay of ^{235}U. The other heavy elements, including plutonium and thorium, exhibit similar chains of radioactive decay which terminate in stable elements.

Since all nuclear materials of interest are naturally radioactive, the mere presence of measurable amounts of radioactivity from a sample does not uniquely define the contents of that sample. A closer look must be taken at the specific nature of the emitted radiation in order to utilize the differences in the natural radioactivity from different elements for the purpose of assaying the sample. This document will be limited to a more detailed inspection of the gamma radiation emitted from nuclear materials and of how its measurement can be useful for Safeguards assay work. Discussions of the methods and utility of measuring the neutron, beta and alpha radiation from nuclear material samples are available elsewhere.

Gamma-rays emitted from nuclear material have two distinguishing characteristics, their energy and intensity. The specific energies and intensities (usually referred to as the gamma-ray spectrum) differ substantially from one nuclear material to the next. For example,

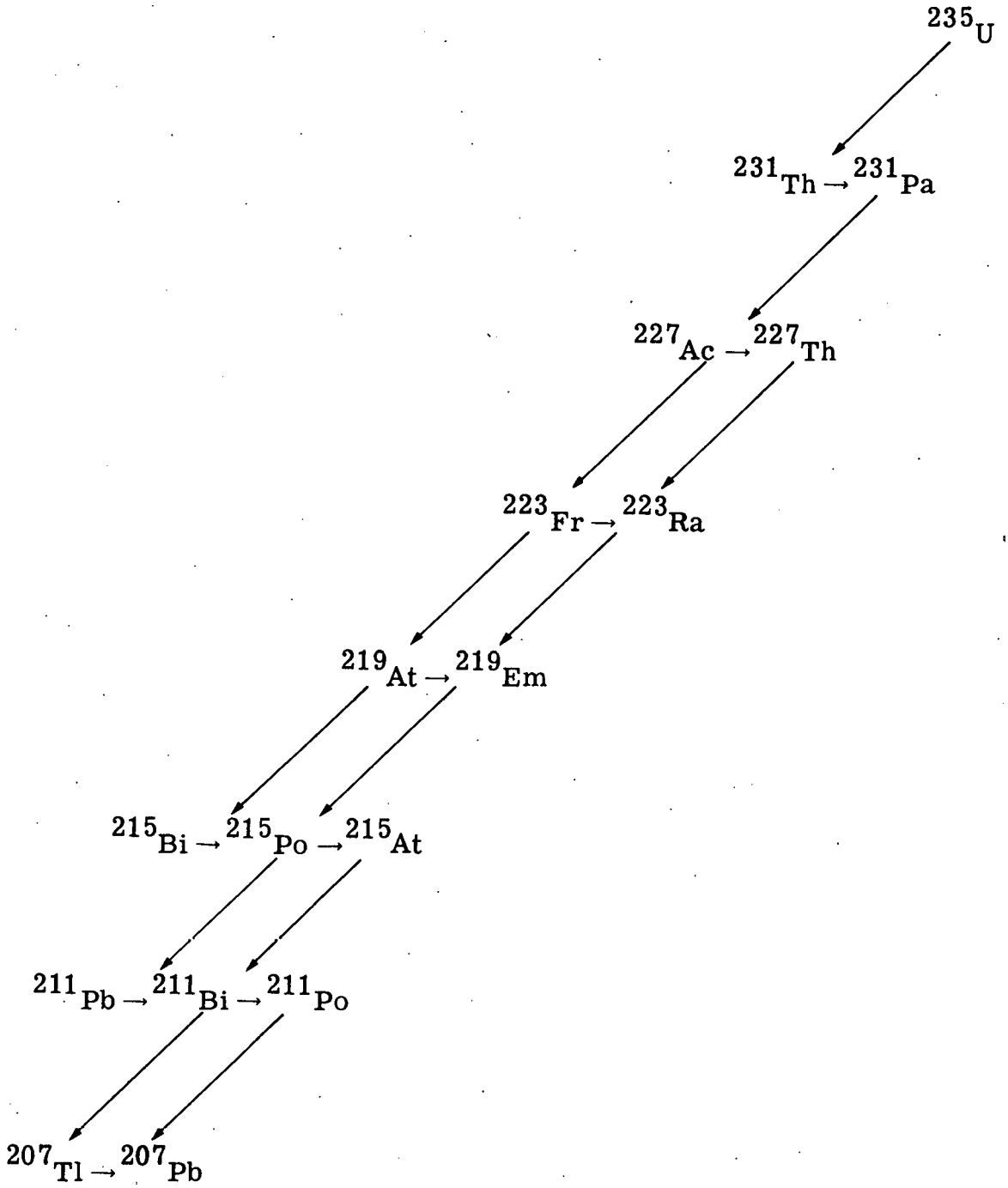

Fig. 1-1. Natural radioactive decay chain for the actinium series. Decay radiation and half lives for the various steps in the chain are given in Table 1.1.[34]

TABLE 1.1

THE ACTINIUM SERIES OF RADIOACTIVE DECAY [34]

Isotope	Type of Disintegration	Half-Life
^{235}U	α, γ	7.10×10^{8} y
^{231}Th	β, γ	25.6 h
^{231}Pa	α, γ	3.43×10^{4} y
^{227}Ac	α, β, γ	21.6 y
^{227}Th	α, γ	18.17 d
^{223}Fr	α, β, γ	22 m
^{223}Ra	α, γ	11.68 d
^{219}At	α, β, γ	0.9 m
^{219}Em	α, γ	3.92 s
^{215}Bi	α, β, γ	8 m
^{215}Po	α, β, γ	1.83×10^{-3} s
^{211}Pb	β, γ	36.1 m
^{215}At	α, γ	10^{-4} s
^{211}Bi	α, β, γ	2.15 m
^{211}Po	α, γ	0.52 s
^{207}Tl	β, γ	4.79 m
^{207}Pb	Stable	

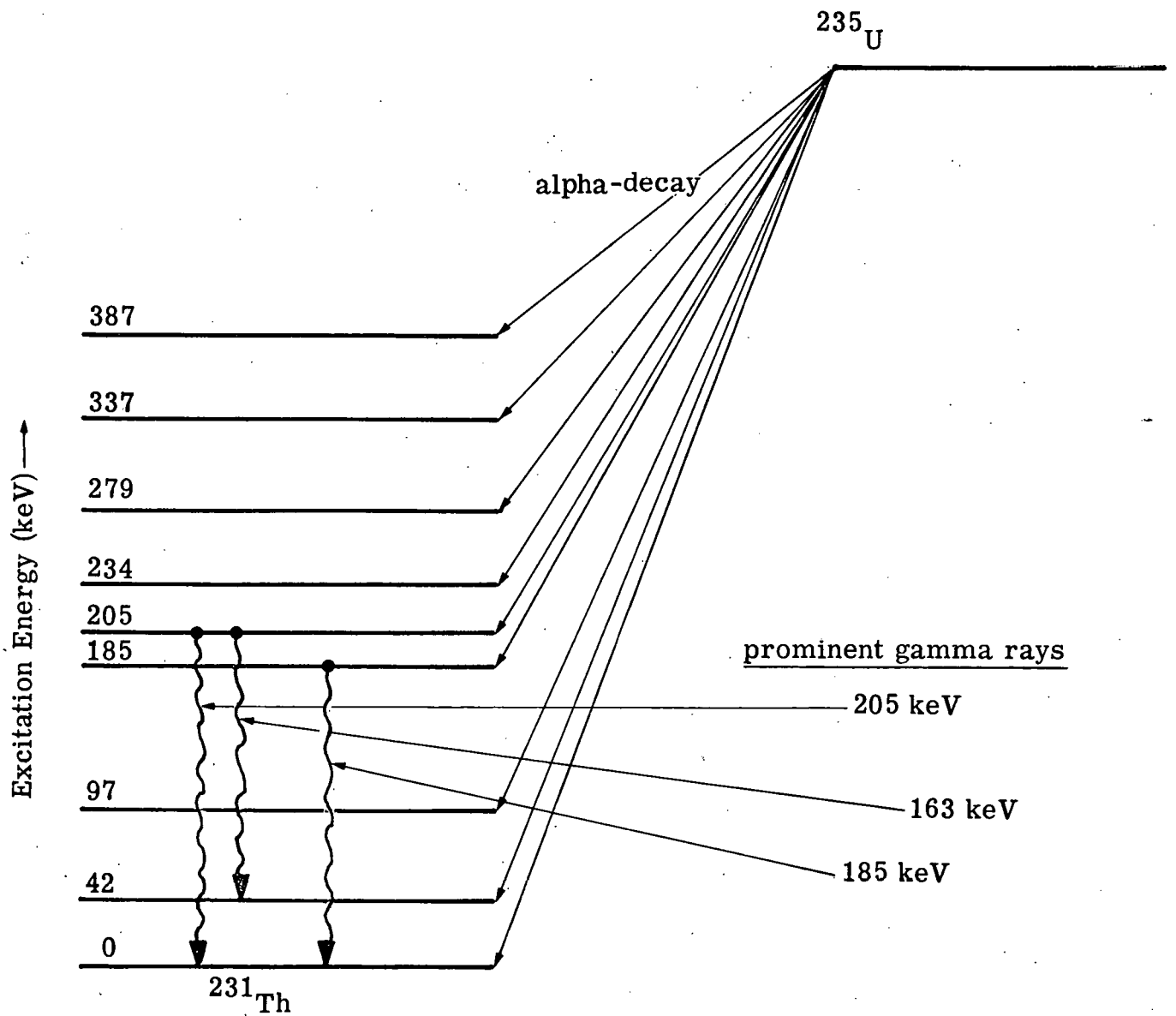

Fig. 1.2. Energy level diagram showing the origin of several prominent gamma rays following the alpha decay of ^{235}U. Alpha decay of ^{235}U can leave the residual ^{231}Th nucleus with an excess of energy; the "excited" ^{231}Th nucleus rids itself of this excess energy and passes to a less excited state by the emission of a gamma ray. Similar diagrams could be drawn for each step in the decay chain illustrated in Fig. 1.1.[35]

TABLE 1.2

ENERGIES AND INTENSITIES OF RELATIVELY INTENSE GAMMA-RAYS EMITTED FROM SAMPLES OF ^{235}U AND ^{239}Pu WITH E_γ * GREATER THAN 130 keV

(Reference 11)

^{235}U	^{239}Pu	E_γ (keV)	Intensity (gamma-rays per 100 disintegrations)
X		163.4	4.6
X		185.7	54.0
X		205.3	5.0
	X	375.0	.015
	X	413.7	.015

* E_γ is the gamma-ray energy.

the energies and intensities of several of the more intense gamma-rays emitted from ^{235}U and from ^{239}Pu are given in Table 1.2

From the table above, it is evident that the energies and intensities of the prominent gamma-rays from ^{235}U are quite different when compared to those from ^{239}Pu. Thus, a device which measures the gamma spectrum emitted from a sample of nuclear material can, in principle, be used to infer the amount of ^{235}U and ^{239}Pu present in the sample. Under ideal conditions, one can further argue that assays of all nuclear materials in the fuel cycle are possible using previously measured gamma spectra data. In other words, a measurement of the

gamma spectrum (the intensity and energy of the gamma-rays) emitted from a sample of nuclear material can be used to detect the amount and type of material present in the sample.

Complexities in actual measurements associated with self-absorption, high radiation backgrounds from irradiated material, and awkward sample configurations will not be considered here. These very real problems can place limits on the effectiveness of gamma-ray assay techniques in certain situations. A number of detailed studies have been made and others are still in progress to develop techniques and instrumentation for solving specific gamma assay problems. Detailed records of the results of these Safeguards studies are available in the literature. The present treatment of gamma assay is meant to serve only as a simple introduction to the methods of using gamma-ray measuring equipment in Safeguards assay work. With this aim in mind, the remainder of this document will be devoted to a description of the two devices considered to be most useful for measuring gamma-ray spectra from samples of nuclear material.

2. A Ge(Li) DETECTOR FOR GAMMA-RAYS

2.1 Theory of Operation

A typical lithium drifted germanium (Ge(Li)) detector for gamma-rays can be represented simply as a cooled cylinder of solid, high resistivity material with a high voltage applied between the outer surface and the central core (Fig. 2.1).

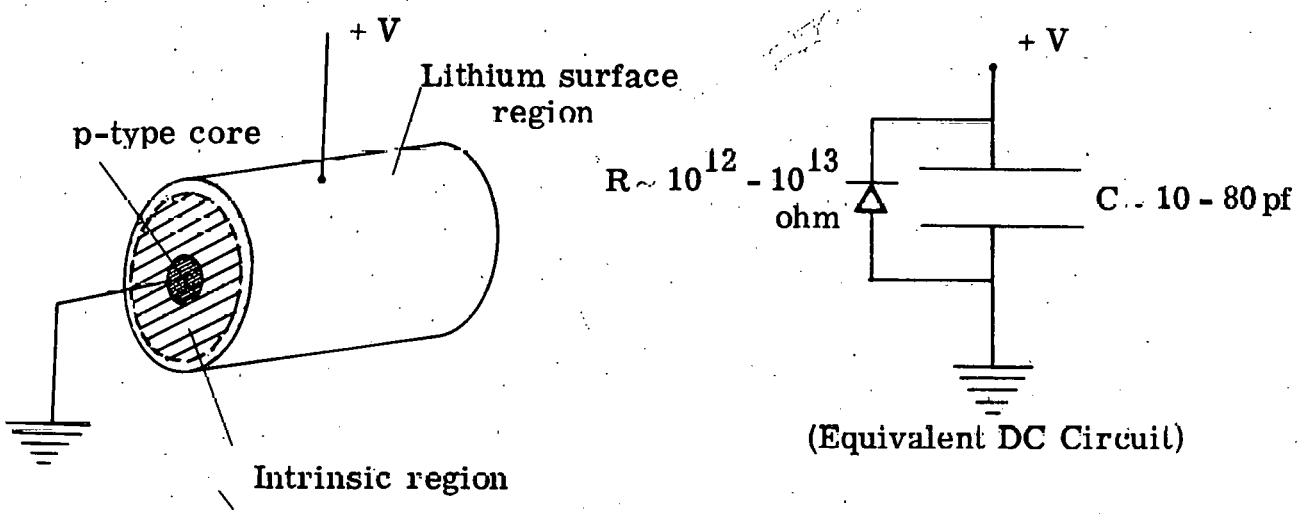

Fig. 2.1. Ge(Li) detector.

Germanium crystals are typically available with impurity concentrations of about 10^{13} to 10^{14} impurities/cc. Large numbers of crystal impurities cause

excessive leakage currents when voltage is applied across the detector. They also act to "quench" the signals produced in the detector by a process called "trapping." These problems caused by impurities can be effectively overcome by a compensating technique called "lithium drifting."

Lithium drifted germanium (Ge(Li)) detectors are made by first evaporating a lithium film on the outer surface of a cylinder of p-type germanium. This lithium film is absorbed into the surface region at about 400°C to create an n-p junction (or diode) at the lithium/p-type germanium interface. Some of the lithium is then diffused into the p-type germanium by applying a bias of several hundred volts across the junction and raising the temperature of the germanium to about 20°-50°C. The lithium ions drift in the applied electric field toward the center of the cylinder in such a way as to compensate the germanium impurities and an "intrinsic" region with an apparent impurity concentration of about 10^{10} impurities/cc is created. At liquid nitrogen temperatures (-196°C), a voltage in the range of 800-5000 volts can be applied across the intrinsic region (which can have a volume greater than 100 cc) with very little leakage current. Electrically the device resembles a solid dielectric capacitor where the intrinsic region represents the solid dielectric.

Electric field strengths of 50-200 volt/mm can typically be maintained across the intrinsic region.

It should be noted that the high resistance across the detector is the result of a diode characteristic. Hence, the resistance observed across the intrinsic region is very low if a bias is applied with a polarity opposite to that which is shown.

Gamma-rays (high energy electromagnetic radiations) incident on the detector can interact in the intrinsic region by any of three different processes: photoelectric absorption, Compton collision, or pair production. All of these processes produce ionization and free charge in the intrinsic region. Gamma-rays are detected by measuring the free charge collected at the electrodes by the high voltage applied across the intrinsic region (Fig. 2.2).

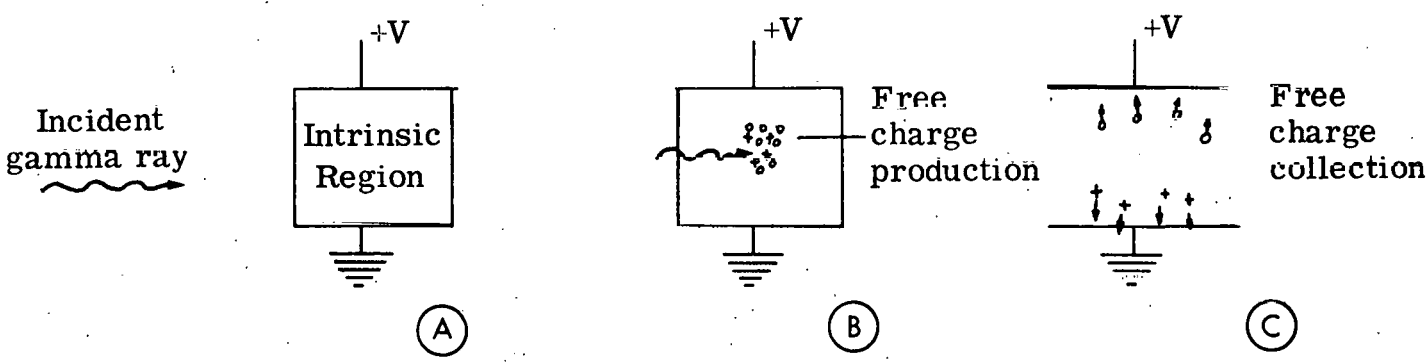

Fig. 2.2. Sequence of events for gamma detection with Ge(Li) detector.

Let us now take a closer look at the gamma interaction processes which produce this free charge.

Photoelectric Absorption

In a photoelectric interaction, the entire energy of the incident gamma-ray is absorbed by a bound atomic electron in the intrinsic material and the gamma-ray disappears. This electron is now set free with a kinetic energy equal to the gamma-ray energy minus a small amount due to the binding energy of the electron. This energetic free electron creates additional ionization and produces free charge in the intrinsic region until all of the initial gamma-ray energy has been used up in the ionization process. The total amount of free charge created is directly proportional to the energy of the initial gamma-ray. The process is depicted in Fig. 2.3, and the number of free charge pairs produced is given in Eq. 2.1.

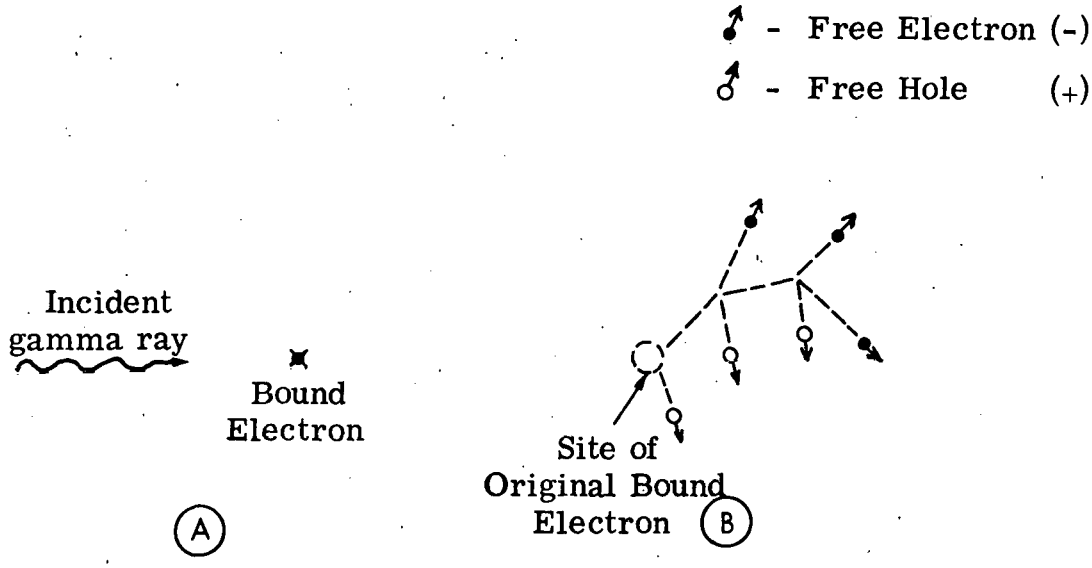

Fig. 2.3. The photoelectric absorption process.

$$n = \frac{E_\gamma}{\epsilon} \quad , \tag{2.1}$$

where n = number of free charge pairs produced (1 free charge pair = 1 electron + 1 hole),

E_γ = initial gamma energy (electron volts),

ϵ = average energy required to create a free charge pair (2.9 eV in germanium).

Compton Scattering

In the Compton scattering interaction, the incident gamma-ray scatters off a bound electron in the intrinsic region and transfers a fraction of its energy to it which is sufficient to set it free. The free energetic electron then ionizes other atoms in the region until all of the transferred energy has been expended in ionization. The scattered gamma-ray may either escape from the detector or interact again. If the scattered gamma-ray escapes, the amount of ionization produced is proportional to the fraction of energy which is initially transferred to the bound electron. This can be any amount up to a well defined upper limit which is less than the incident gamma-ray energy. There is therefore, a continuous distribution of possible amounts of free charge which can be created by this process from essentially zero up to a calculable maximum. Mathematically,

$$n = 0 \text{ to } \frac{E_{max}}{\epsilon} \quad , \tag{2}$$

where

$$E_{max} = E_\gamma \frac{1}{1 + \frac{m_o c^2}{2E_\gamma}} \quad . \tag{2.3}$$

$m_o c^2$ = rest mass of the electron (0.511 MeV).

The process is depicted in Fig. 2.4.

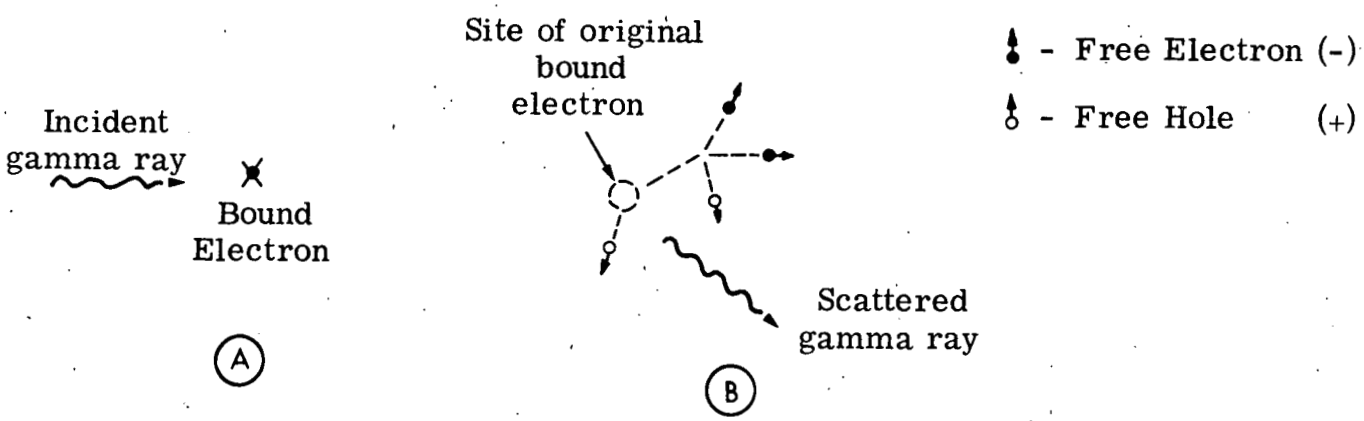

Fig. 2.4. The Compton scattering process.

Pair Production

If the incident gamma-ray energy is greater than $2 m_o c^2$ (1.022 MeV), then pair production is a third possible interaction process. The incident gamma-ray converts its energy into an energetic positron-electron pair and the gamma-ray disappears. These two particles lose their kinetic energy (equal to $E_\gamma - 2 m_o c^2$) by ionization. After slowing down, however, the positron will react quite readily with ordinary electrons in

the detector. In this process, called annihilation, both the positron and an electron disappear and two 511 keV gamma-rays are formed moving in opposite directions from one another. Usually both these 511 keV gamma-rays escape from the intrinsic region of the detector so that the free charge produced is proportional to (E_γ - 1.022 MeV), or

$$n = \frac{(E_\gamma - 1.022\ \text{MeV})}{\epsilon} \tag{2.4}$$

The process is depicted in Fig. 2.5 and is referred to as "double escape".

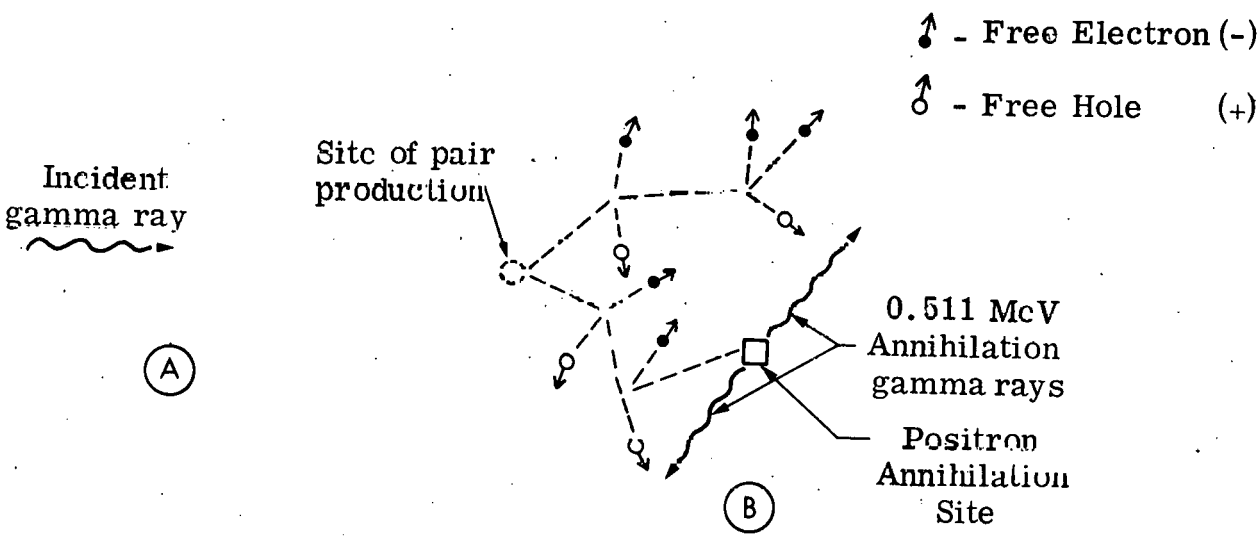

Fig. 2.5. Pair Production

Multiple Processes

The interaction of a gamma-ray with the detector can also involve various combinations of the three simple gamma-ray interactions

described previously. The total charge available for collection from these multiple processes will be equal to the sum of that created in each of the individual processes.

For example, consider again the case of Compton scattering. After the incident gamma-ray has scattered once, it can interact again in the intrinsic region (for example, by the photoelectron absorption process) so that all the initial incident gamma-ray energy is converted into ionization in two steps. Thus, this multiple step process would produce as much free charge as a single photoelectric interaction of the initial incident gamma-ray. Similarly, in the case of pair production, both 511 KeV gamma-rays could also be absorbed within the intrinsic region and thus ionize a number of atoms proportional to E_γ. In general, therefore, for full energy absorption by multiple processes such as those described above,

(Full energy absorption.) $$n = \frac{E_\gamma}{\epsilon} . \qquad (2.5)$$

Another process resulting in a well defined amount of ionization is pair production followed by absorption of only one of the 511 keV annihilation gamma rays. This is commonly referred to as "single escape" and the amount of free charge produced is proportional to $(E_\gamma - 0.511\ \text{MeV})$ or,

(Single escape) $$n = \frac{(E_\gamma - 0.511\ \text{MeV})}{\epsilon} \qquad (2.6)$$

The full energy absorption multiple processes described above result in the production of a well defined amount of ionization. On the other hand, other multiple processes result in a continuous distribution for the amount of ionization produced. (Examples: (1) pair production followed by the escape of one 511 keV gamma ray after it has Compton scattered once, (2) two Compton scatterings followed by the escape of the twice scattered incident gamma ray.) Events such as these are similar in effect to single Compton scattering which also exhibits a continuous distribution for free charge production.

Having considered the gamma interaction process in some detail, let us now focus attention on the effects of the ionization produced. The products of the ionization created by incident gamma-rays interacting in the intrinsic regions are positive (holes) and negative (electrons) free charges. These free charges are separated by the electric field applied across the intrinsic region, and collected at the electrical contacts. The time required to collect this free charge is on the order of 10 to 100 nanoseconds (10^{-8}-10^{-7} seconds), depending on the exact geometry of the detector and the applied voltage. Thus, the detection of a gamma-ray is signified by a small current pulse which can be measured with appropriate external circuitry. The Ge(Li) detector operates like a solid-state analogue of the well known gaseous ionization chamber.

The total charge contained in this current pulse depends on the energy of the gamma-ray and the type of interaction which has taken place. The equations for the average amount of ionization (and hence, the average number of free charges of either sign) were given earlier and are collected together below for easy reference.

$$n = \frac{E_\gamma}{\epsilon} \qquad \text{(photoelectric absorption and full energy absorption multiple processes)} \qquad (2.1) \text{ and } (2.5)$$

$$n = 0 \text{ to } \frac{E_{max}}{\epsilon} \; ; \quad E_{max} = \frac{E_\gamma}{1 + \frac{m_o c^2}{2E_\gamma}} \qquad \text{(Compton Scattering)} \qquad (2.2); \; (2.3)$$

For E_γ greater than 1.022 MeV, in addition to the above:

$$n = \left(\frac{E_\gamma - 1.022 \text{ MeV}}{\epsilon}\right) \qquad \text{(pair production - double escape)} \qquad (2.4)$$

$$n = \left(\frac{E_\gamma - 0.511 \text{ MeV}}{\epsilon}\right) \qquad \text{(pair production - single escape)} \qquad (2.6)$$

The average energy required to create a free charge pair in germanium (ϵ) is 2.9 eV. Thus, one can calculate the average amount of free charge produced in the different interactions. Results for 1 and 2 MeV gamma-rays are shown in Table 2.1.

TABLE 2.1

AVERAGE AMOUNT OF CHARGE (NEGATIVE OR POSITIVE) PRODUCED BY 1 AND 2 MeV GAMMA-RAY INTERACTIONS IN A Ge(Li) DETECTOR.

Process	1 MeV gamma-ray	2 MeV gamma-ray
Photoabsorption and Multiple Processes resulting in full energy absorption	5.50×10^{-14} C*	1.10×10^{-13} C
Compton Scattering	0 to 4.40×10^{-14} C	0 to 9.75×10^{-14} C
Pair Production - double escape	not applicable	5.40×10^{-14} C
Pair Production - single escape	not applicable	8.20×10^{-14} C

These charges correspond to peak currents in the microamp (10^{-6}a) region so that sensitive electronic amplifiers must be used to raise the signal level to values which can be conveniently recorded. If the number of pulses are recorded as a function of their amplitude, spectra similar to those shown in Fig. 2.6 and Fig. 2.7 result Figure 2.6 is a spectrum from a source of 662 keV gamma rays (^{137}Cs) and Fig. 2.7 is the upper portion of a spectrum from a source of 2.61 MeV gamma rays (^{208}Tl). It should be noted that for photoabsorption, full energy absorption, and single and double escape processes, a sharp peak is observed in the pulse height spectrum. The position of the peak in the

*C = Coulomb

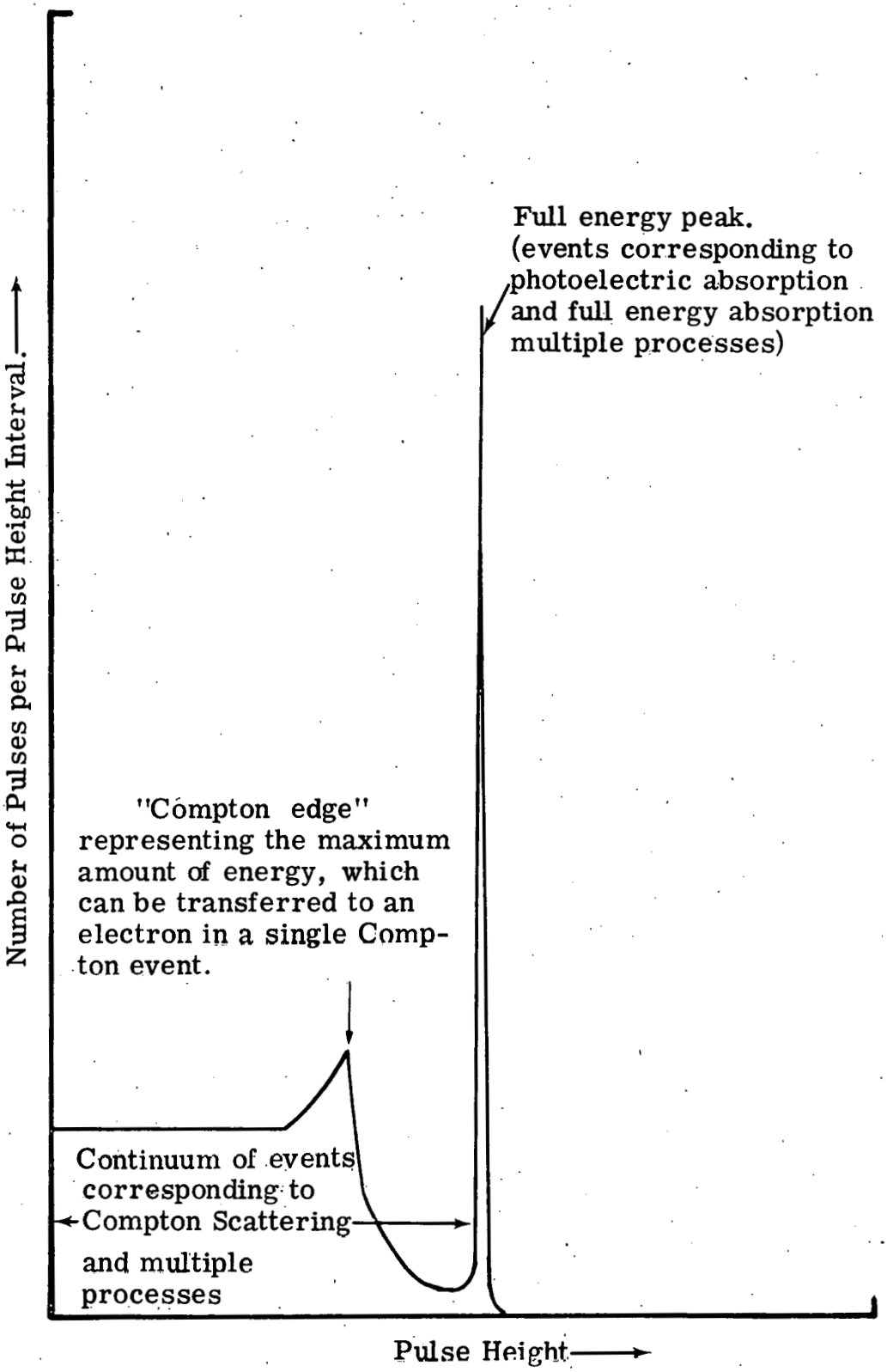

Fig. 2.6. Ge(Li) detector pulse height spectrum from monoenergetic 662 keV incident gamma rays.

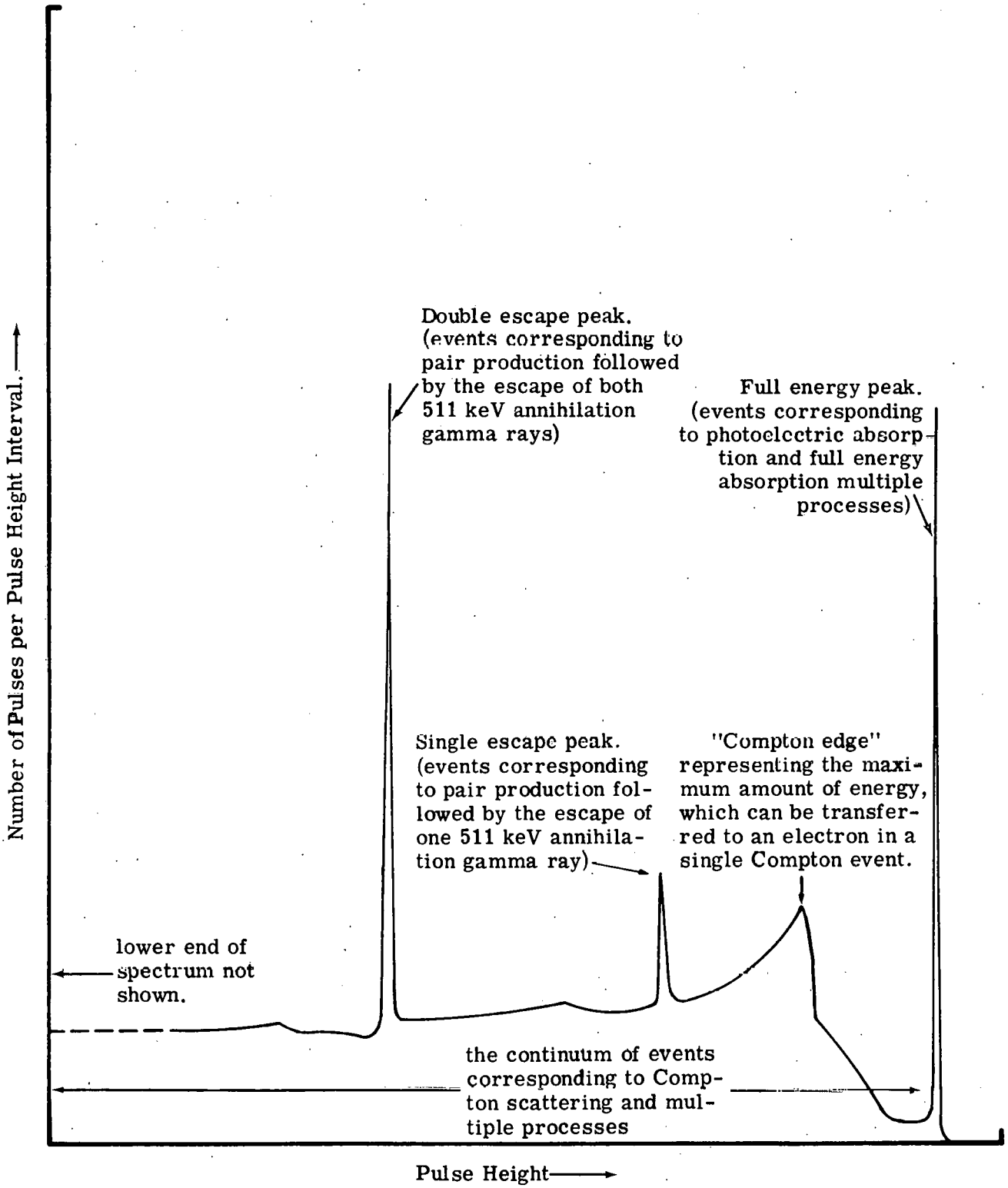

Fig. 2.7. Ge(Li) detector pulse height spectrum from monoenergetic 2.61 MeV incident gamma rays.

spectrum is directly related to the gamma-ray energy, and the number of counts in the peak is directly related to the intensity of the incident gamma-rays. The Compton scattering events (and certain multiple process events) constitute a continuous background which must be subtracted from the useful data in the peaks.

The maximum amount of energy which can be transferred to an electron by an incident gamma ray in a Compton scattering event (E_{max}) is also evident in the spectra and is referred to as the "Compton edge."

$$E_{max} = \frac{E_\gamma}{1 + \frac{m_o c^2}{2E_\gamma}} \qquad (2.3)$$

The events recorded between the Compton edge and the full energy peak correspond to gamma rays which have Compton scattered more than once and then escape from the detector. They also correspond to gamma rays which have undergone small angle scattering in the source, in the can surrounding the detector, or in the small dead space at the surface of the detector, followed by full absorption. Actually this has the effect of making the full-energy peak asymmetric, and of creating a "tail" on the low energy side of the peak. In Fig. 2.7, where the incident gamma rays

have an energy greater than 2 $m_o c^2$, the events between the Compton edge and the full energy peak can also correspond to pair production events followed by Compton scattering of one or both of the annihilation gamma rays before their escape from the detector.

From the simple description of the operation of Ge(Li) detectors, it is obvious how they can be used in Safeguards assay applications. The measured spectra exhibit distinguishable peaks corresponding to the energy and intensity of the gamma-rays incident on the detector. If the pulse height spectrum has been previously calibrated with standard samples, the Ge(Li) detector can be used to identify and quantify the different nuclear materials by comparing the spectra from unknown samples with spectra from standard samples of known content.

2.2 Description of Ge(Li) Detection Systems

Practical Ge(Li) gamma-ray detector systems consist of the following components:

(A) lithium drifted germanium crystal,

(B) liquid nitrogen cooling system and vacuum system,

(C) detector electronics (preamplifier, main amplifier, and pulse height analyzer).

(A) Lithium Drifted Germanium Crystals

The lithium drifted germanium crystals are made in two basic geometries - planar and coaxial. Simplified sketches of these two geometries are shown in Fig. 2.8 together with several variations of the coaxial geometry. The coaxial detectors are useful for many Safeguards assay applications because they can be made with larger intrinsic volumes, and hence, greater efficiency. Smaller planar devices, however, can be useful for applications requiring extremely good energy resolution and for measurements of low energy gamma-ray spectra. Intrinsic volumes of up to 120 cc are available commercially.

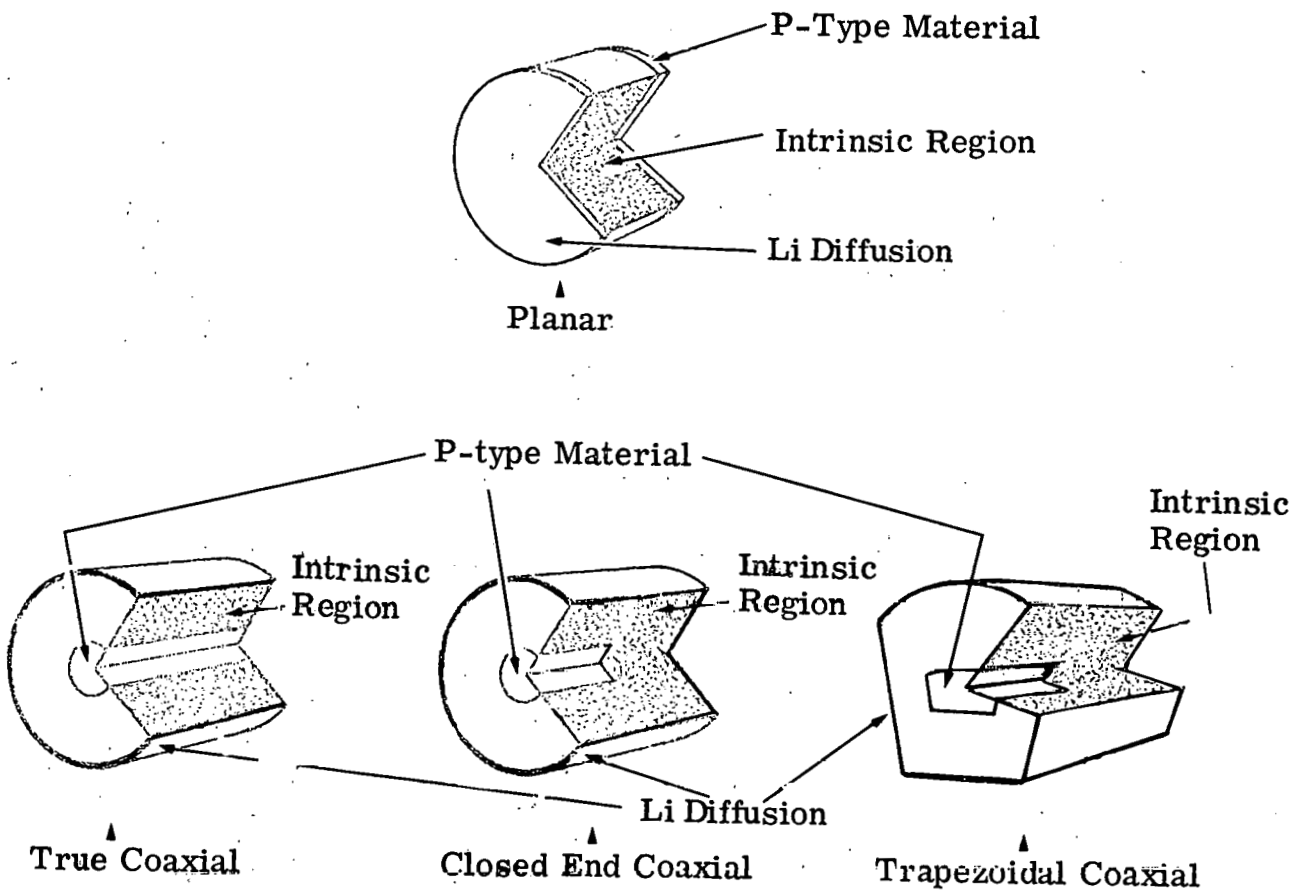

Fig. 2.8. Planar and coaxial Ge(Li) detectors.

(B) Liquid Nitrogen Cooling System and Vacuum System.

In order for the Ge(Li) crystal to work properly with low leakage currents, it must be kept at liquid nitrogen temperatures (-196°C). To prevent condensation from forming on the cooled crystal and to eliminate effects from impurities in the atmosphere, the crystal is packaged in an evacuated container. A method of cooling commonly used is to mount the crystal on a dip-stick which extends down into the liquid nitrogen. Another cooling configuration is the "chicken feeder" or gravity feed system. Typical cooling and vacuum systems for a Ge(Li) detector are shown in Fig. 2.9. Dewars, containing the liquid nitrogen, typically require replenishment from 1 to 3 times a week (depending on their size). The vacuum in the crystal container is maintained by using a molecular sieve (which must be rejuvenated at 10 to 12 month intervals) and/or a small vac ion pump which operates from a 110 VAC electrical supply. The molecular sieve and vac ion pump are effective in maintaining the vacuum between 10^{-4} and 10^{-7} mm Hg. If for any reason the vacuum is allowed to deteriorate to levels above about 10^{-2} mm Hg, a mechanical roughing pump must be used to re-evacuate the container.

In normal operation, routine maintenance of the cooling and vacuum system consists of replenishing the liquid nitrogen supply.

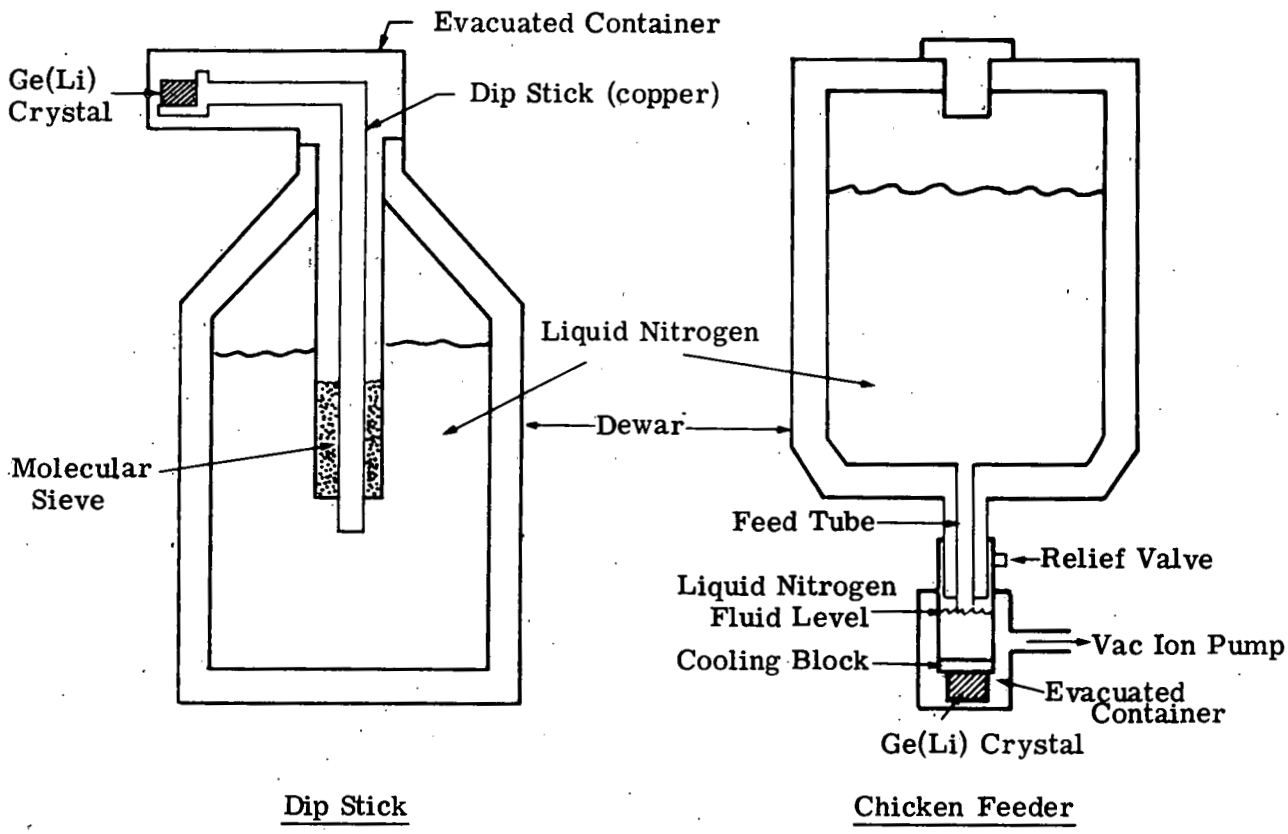

Fig. 2.9. Typical Ge(Li) cooling and vacuum systems.

Vacuum gauges are sometimes provided by the manufacturer in order to insure that the vacuum is being properly maintained. Except for cases of unexpected malfunction or replacement of the molecular sieve, there is no reason to disturb the vacuum integrity of the crystal container.

(C) Detector Electronics

The small pulses from the Ge(Li) crystal must be amplified and shaped, and the information stored in a convenient form to facilitate handling of the data. A block diagram of the basic electronic system used for accomplishing this is shown in Fig. 2.10.

The preamplifier is physically located as close as possible to the Ge(Li) crystal in order to minimize preamplifier noise. The preamplifier integrates the detector current and is used to drive the main amplifier which can be operated at a more remote location. For systems requiring extremely good resolution, the preamplifier can be mounted directly on the cryostat and the field effect transistor (FET) in the first amplifying stage can be cooled to liquid nitrogen temperatures. This configuration is referred to as a "cooled FET" preamp.

The main amplifier is used to shape the pulse in order to optimize the signal to noise ratio, compensate for high count rates,

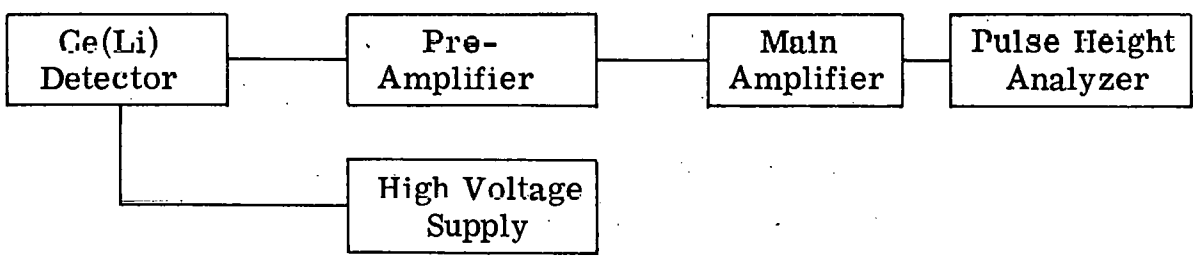

Fig. 2.10. Block diagram for detector electronics.

and further amplify and tailor the pulse for input to the pulse height analyzer. The pulse height analyzer is used to sort the incoming pulses according to pulse height into a number of discrete energy bins or channels. The number of channels available depends on the particular model, but somewhere between 400 to 4000 channels are commonly used. A well regulated high voltage supply (typically 0-5000 V) is used to bias the detector. Additional components which are useful for monitoring the condition of the detector are a nanoammeter for measuring the detector leakage current and an ion gauge for measuring the container vacuum.

2.3 Performance Characteristics of Ge(Li) Systems

There are two basic characteristics of a Ge(Li) system which are important considerations when evaluating its performance in Safeguards nuclear material assay applications. These are:

(A) Energy resolution

(B) Efficiency

(A) Energy Resolution

The most commonly used figure of merit for the energy resolution of the system is the full width of a peak in the spectrum at half its height (FWHM) (Fig. 2.11). In addition, the full width of the peak at 1/10 its height (FW1/10M) is also quoted in some publications (Fig. 2.11).

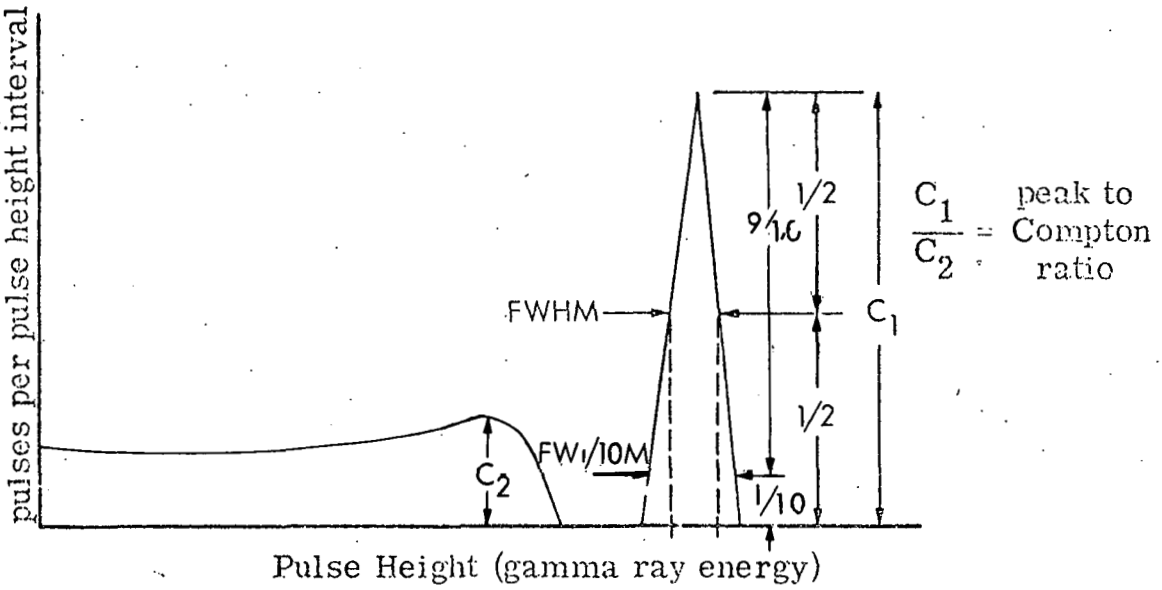

Fig. 2.11. Full Width at Half Maximum (FWHM), Full Width at 1/10 Maximum (FW1/10M) and peak to Compton ratio - defined.

The energy resolution for Ge(Li) detectors is at least ten times better than that which can be obtained with NaI detectors or other commonly used systems. It is important, therefore, to take maximum advantage of the excellent resolution afforded by the Ge(Li).

Two gamma spectra taken with the same Ge(Li) system are shown in Fig. 2.12. The spectrum at the top of the figure was taken with a system whose parameters were not optimized for obtaining the best resolution — the lower spectrum was taken with the same system optimized. It is clear that the better resolution afforded by an optimized system gives a significantly greater amount of useful information. In

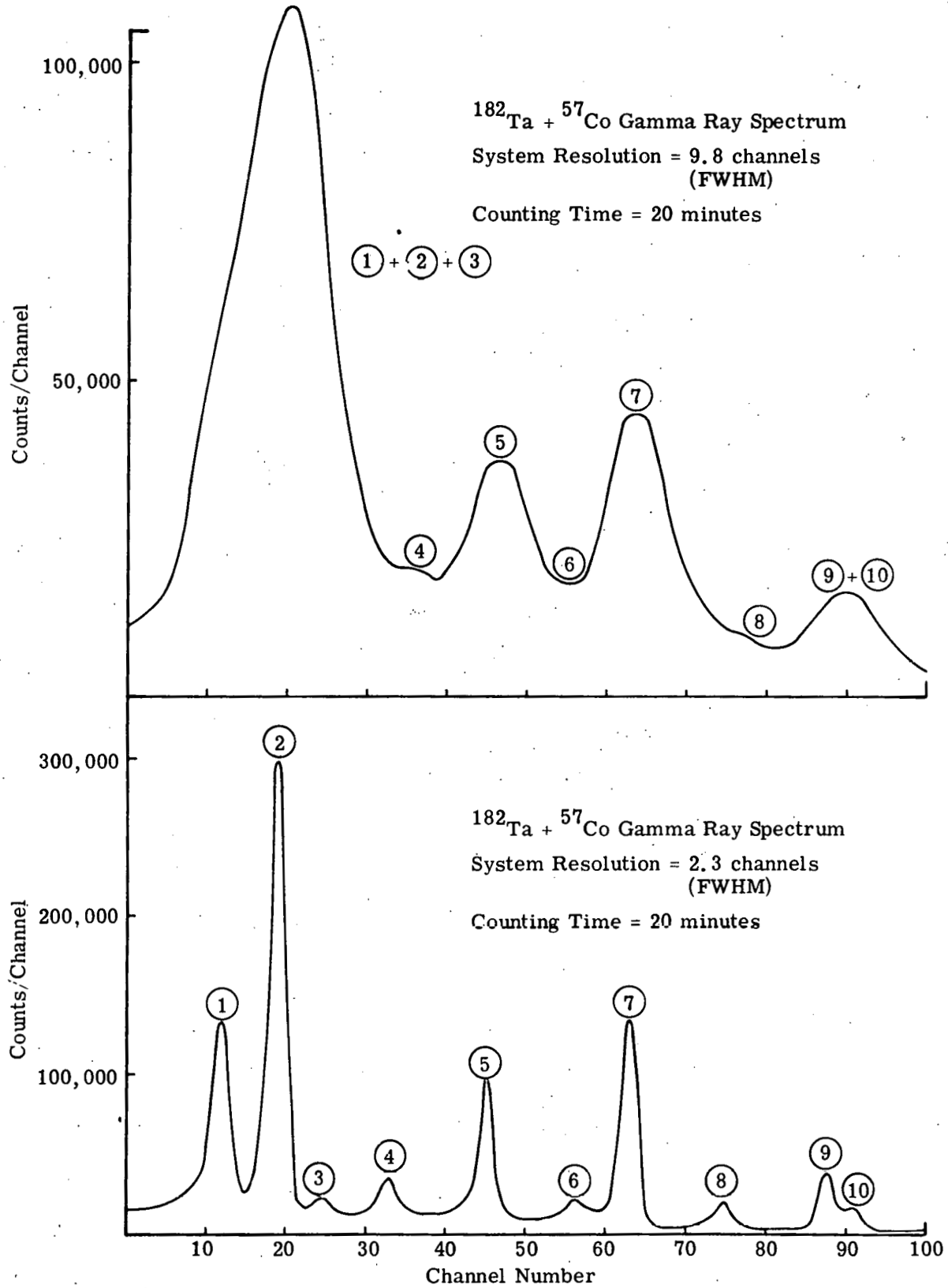

Fig. 2.12. Examples of spectra taken with the same Ge(Li) system, operated with different energy resolutions.

particular, if the peak labeled (2) was the peak of interest, and the peaks labeled (1) and (3) were contaminants, a system with poor resolution would not detect the contaminants and an erroneous number of counts would be assigned to the intensity of peak (2). Also, weak signals such as peak (6) would not even be detected in the system with poorer resolution. Some of the more common sources of peak broadening (or deterioration of the system resolution) will be briefly discussed below.

The fact that any peak does not have a "zero" width (FWHM = 0) is due to several factors:

1) The production of free charge by an incident gamma-ray is a statistical process, hence there are fluctuations in the amount of charge created by gamma-rays of a given energy. This contributes to a minimal intrinsic peak width which is estimated to be given by

$$\text{FWHM (keV)} \simeq 1.4 \sqrt{E_\gamma \text{ (MeV)}}.$$

The intrinsic resolution versus energy is shown in Fig. 2.13.

2) If the high voltage applied to the detector is too large, the leakage current (or noise) may be large enough to be a significant factor in degrading the system's resolution. High leakage currents may also develop due to

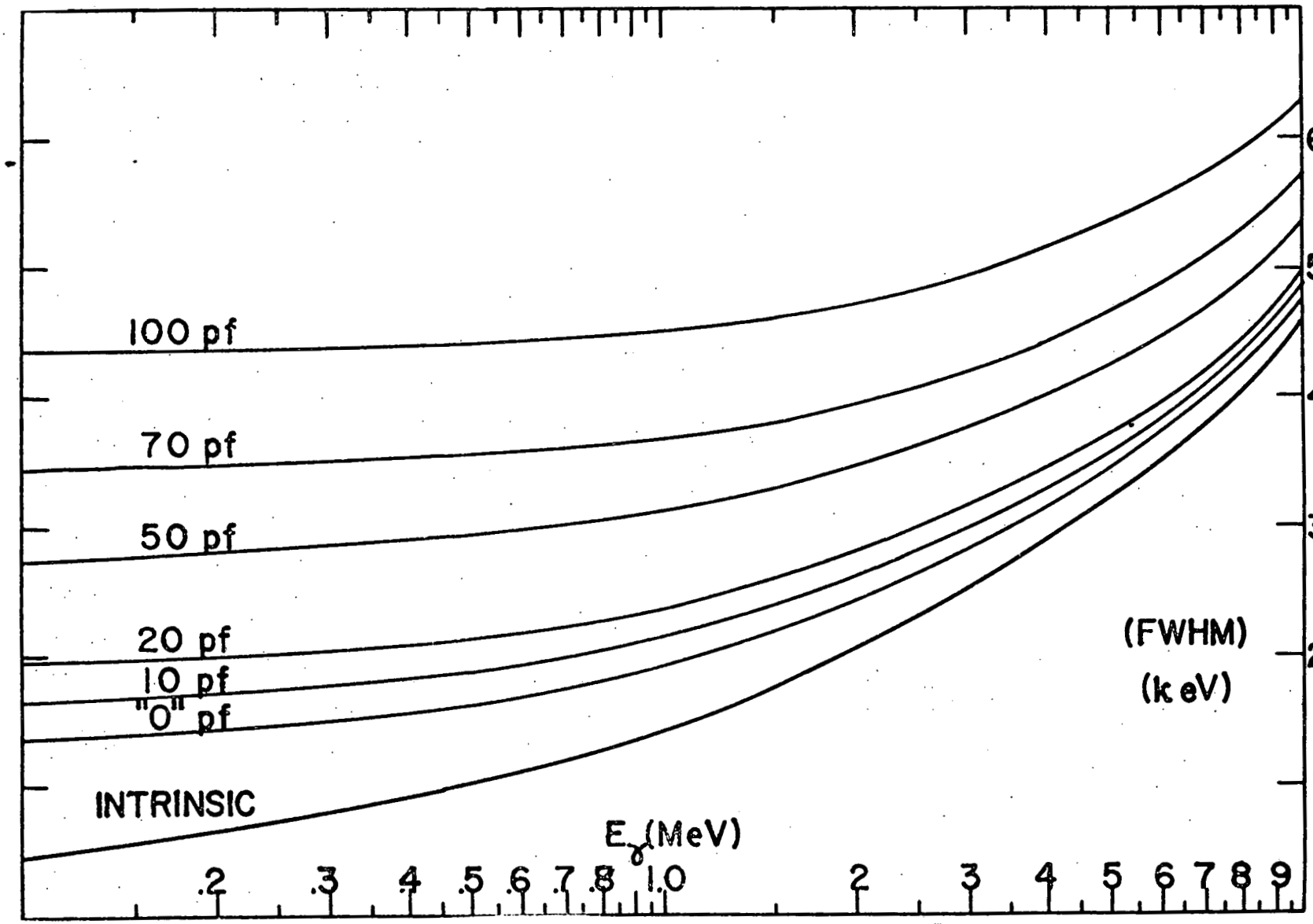

Fig. 2.13. Ge(Li) system energy resolution versus gamma-ray energy for different preamplifier input capacitances.[36]

moisture or contamination collecting on the signal cable connectors.

3) The preamplifier also introduces noise into the system and broadens the peak width. This noise is produced by a number of statistical phenomena in the preamplifier components and depends directly on the detector capacitance. The function expressing the dependence of the preamplifier contribution to the FWHM is given below:

$$\Delta E = \Delta E_o + kC_d \qquad (2.7)$$

ΔE = preamplifier contribution to the FWHM of a peak (keV)

ΔE_o = FWHM of a pulser generated peak (no detector attached) (keV).

k = constant (keV/pf)

C_d = detector capacitance (including connections between the detector and preamplifier).

One way to help alleviate this problem is to keep the preamplifier to crystal distance as short as possible, since cables add between 13 to 30 pf/foot and each additional connection adds 2 to 5 pf. An example of the

increase in peak width with increasing input capacitance to the preamplifier is shown in Fig. 2.13. Another important contribution to the system resolution is thermally generated noise in the preamplifier. Therefore, Ge(Li) systems requiring the best resolution available operate critical preamplifier components at low temperature. As an example: at an energy of 1.33 MeV, a preamplifier mounted directly on the cryostat with a "cooled FET" typically contributes half as much to the peak width as a similar system operating at room temperature.

4) The resolution is sensitive to the time constants chosen in the main amplifier, since the main amplifer acts as a filter for some of the noise generated in the preamplifier and detector. The different types of noise sources have different filter requirements, so that the optimal choice of time constants depends on which sources of noise are most important in any given detector system.

5) High counting rates may cause detector pulses to overlap and therefore broaden the system resolution. High counting rates should be avoided if possible by selective shielding, careful positioning of the detector, or pulse

pile-up rejection circuits. A search for the best time constants for any given count rate will also help to minimize the problem. Many amplifiers also contain pole zero cancellation and/or base line restoration circuits which help to maintain good resolution at high count rates. Detailed accounts of recommended procedures for high count rate problems are contained in a number of references.

6) An obvious limit to the resolution of a Ge(Li) system is the use of a pulse height analyzer with too few channels. In order to take advantage of the excellent energy resolution available from Ge(Li) detectors, a sufficient number of channels (5 to 10) should be provided to span the width of a peak of interest. If only a limited number of channels are available and only a portion of the gamma spectrum contains useful information, several techniques are in use for displaying the important portion of the spectrum over the available channels. Some analyzers now on the market have a digital offset capability. This feature allows one to move the zero of the analyzer up to a selected point in the spectrum; then, by adjusting the conversion gain, the remainder of the

spectrum can be expanded over the available channels above this preselected point. Another option available for expanding a certain portion of the spectrum is to use a biased amplifier after the main shaping amplifier; a disadvantage of this method is a slight decrease in the system resolution. Either of the above techniques can be used to eliminate the pulse height analyzer as the limiting factor on the system resolution.

In some cases, Ge(Li) pulse height information has been recorded between lower and upper limits in one broad information channel (commonly referred to as a single channel analyzer). This is only useful if the operator is absolutely confident that all the samples being inspected are identical, since unknown contaminants can result in erroneous readings.

(B) Efficiency

Not all gamma-rays which pass through the detector interact with it. However, as the gamma-ray path length through the detector material lengthens, the fraction which interact within the detector increases. This implies that detectors with larger volumes will exhibit increased efficiency. This leads to shorter assay times and better statistical information. However, the usefulness of larger detectors is even more apparent from the following argument.

The detector efficiency is usually defined as the fraction of incident gamma-rays which deposit all their energy in the detector. This follows since the events recorded in peaks constitute the useful information which can be obtained from the detector response. Since only the photoelectric and certain multiple processes result in the deposition of all the incident gamma-ray energy in the "full energy peak", a better understanding of the efficiency is obtained by looking at the relative probability for each of these processes. Figure 2.14 shows that for gamma-rays with energies less than 150 keV, photoelectric absorption is the dominant interaction, and hence most gamma-rays which interact in the crystal will appear in the full energy peak. Above 150 keV, photoelectric absorption drops rapidly in importance and a significant number of the gamma-rays which appear in the full energy peak are those which have first of all Compton scattered and then been absorbed after one or more subsequent interactions within the detector volume. It is therefore important to use Ge(Li) detectors with larger volumes to enhance the probability for multiple interactions to take place. Stated another way, a larger volume decreases the number of Compton scattered gamma-rays that escape from the detector for gamma-rays in the energy range of 0.2 to 1.5 MeV. The largest volumes presently available are made in the closed end and trapezoid coaxial geometries.

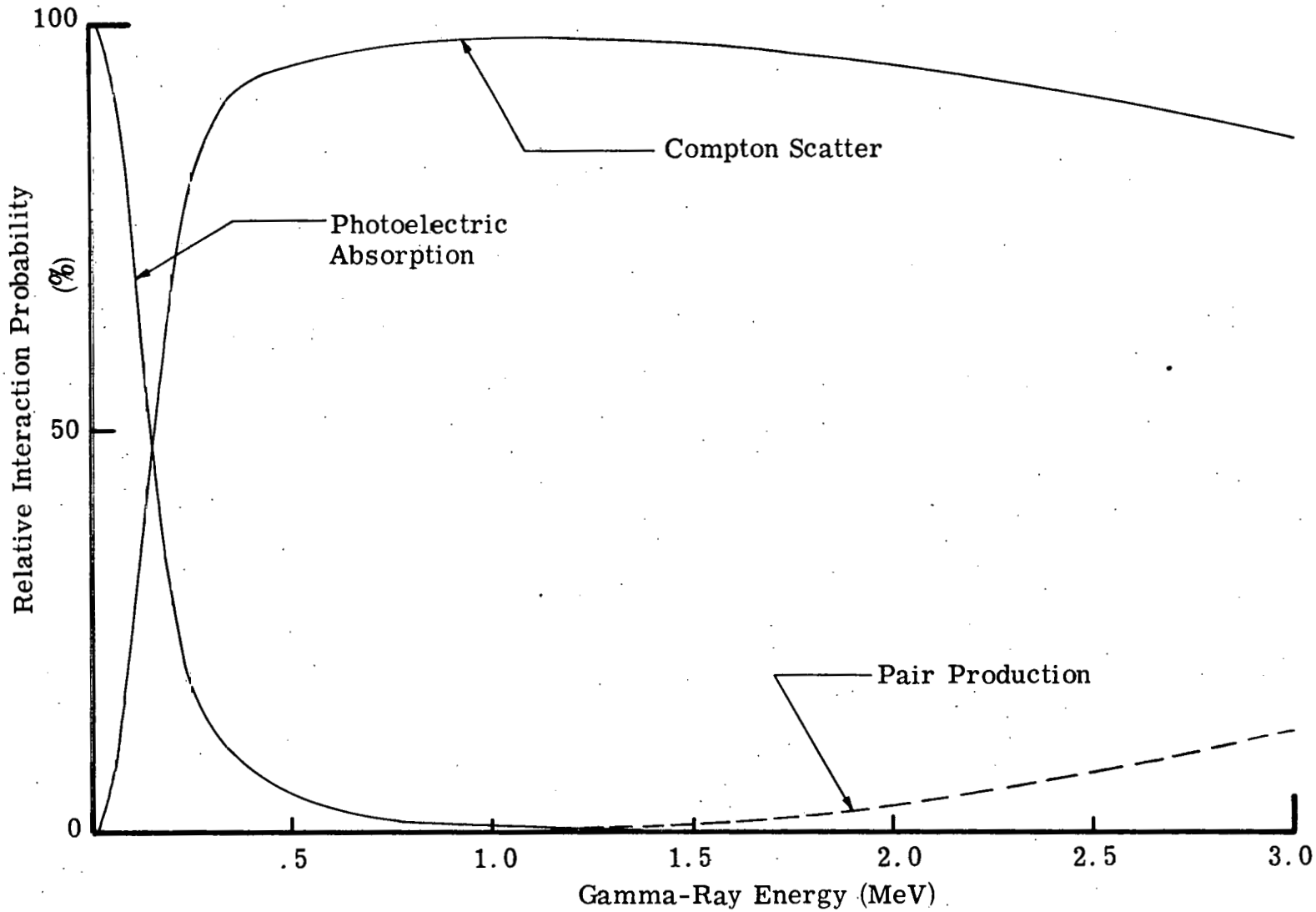

Fig. 2.14. Relative single interaction probabilities for gamma-rays versus energy.[4]

For applications requiring the detection of gamma-rays with energies greater than about 2 MeV, the full energy peak may be very small even for large detectors. However, at these energies it is apparent from Fig. 2.14 that the pair production process is becoming relatively important. Even though this process may not result in an event being recorded in the full energy peak (because of the escape of one or both of the 511 keV annihilation gamma-rays), the event can be recorded in the recognizable single or double escape peaks in the spectrum. The location of these peaks can be easily related to the incident gamma-ray energy (see Fig. 2.15).

Large volume detectors are not the solution to every Safeguards problem. In fact, smaller volume detectors may be optimal for applications requiring the measurement of low energy gamma-rays. In these cases, larger detector volumes may serve only to contribute a larger continuum background from higher energy gamma-rays under the lower energy peaks of interest. In contrast, smaller detectors would have sufficient efficiency for detecting the low energy gamma-rays, but would be relatively transparent to higher energy gamma-rays. Other applications for which smaller (and less expensive) detectors may be suitable are those where high signal levels exist and low count rates are not a problem. The smaller volume detectors are available in the planar geometry.

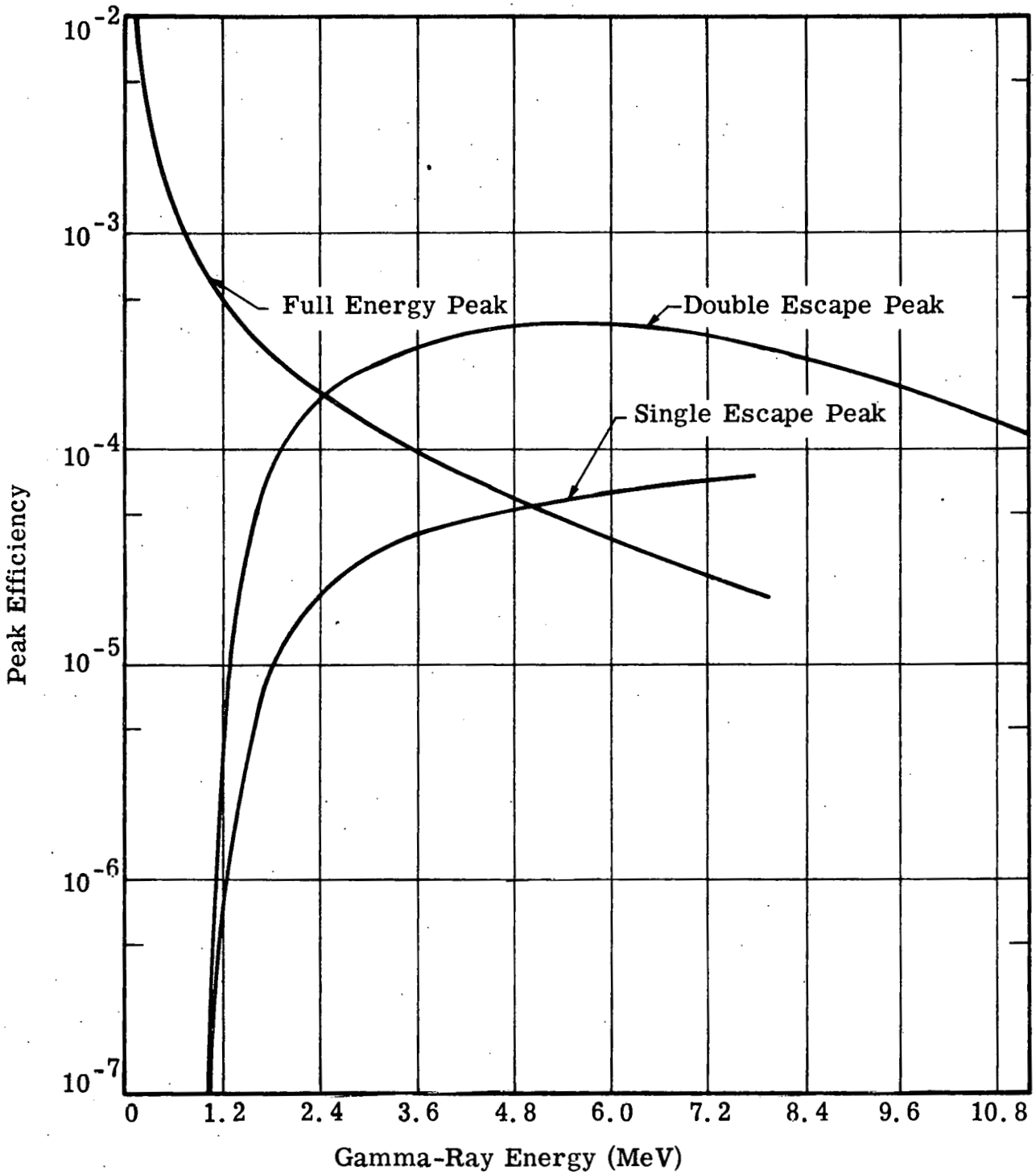

Fig. 2.15. Absolute efficiencies for the full energy, double escape, and single escape peaks versus energy for a 12cc coaxial detector located 3cm from the source. (4)

Three figures of merit for a measure of the Ge(Li) detector efficiency are in common use today. These are listed below:

1) The relative efficiency for the full energy peak in the Ge(Li) spectrum compared to that in a 3" x 3" NaI spectrum. The comparison is made for the ^{60}Co 1.33 MeV full energy peak with the detector located 25 cm from the source. In this comparison, the efficiency used for the NaI crystal can be measured directly or the calculated efficiency given in an established reference can be used.* Because of difficulties in defining the NaI full energy peak, experience has shown that the result obtained for the relative Ge(Li) efficiency is slightly higher when a direct measured comparison between detectors is made as compared to the result obtained using the calculated NaI efficiency.

2) The counting rate in the ^{60}Co 1.33 MeV full energy peak for a calibrated source placed 25 cm from the detector. The relationship between this method of specifying the efficiency and method (1) above can be determined as follows:

The calculated absolute full energy peak efficiency of a 3"x3" NaI detector for the ^{60}Co 1.33 MeV peak is about 1.2×10^{-3} counts per disintegration ($^{cts}/_{d}$). Since 1 μCi

*R. L. Heath, Scintillation Spectrometry Gamma-ray Spectrum Catalogue 2nd Edition 1DO-16880-1 (1964).

corresponds to 3.7×10^4 d/sec, the efficiency of the NaI crystal can be expressed as,

$$3.7 \times 10^{4}\ ^{d}/_{sec \cdot \mu Ci} \times 1.2 \times 10^{-3}\ ^{c}/_{d} = 44\ ^{cts}/_{sec \cdot \mu Ci}$$

The relative Ge(Li) efficiency under the same condition can therefore be written as,

$$\text{Ge(Li) relative efficiency (\%)} = \frac{\text{Ge(Li) 1.33 MeV full energy peak cts/sec} \cdot \mu\text{Ci)}}{0.44} \qquad (2.8)$$

(See Fig. 2.16.)

3) The Peak-to-Compton ratio. The ratio of the full energy peak height to the highest energy portion of the Compton scattering spectrum (see Fig. 2.11). Increases in this parameter reflect: 1) improvements in energy resolution (the same number of counts in a narrower peak imply a greater peak height); and 2) increased efficiency for full energy absorption multiple processes.

Typical values for these parameters, as quoted by detector manufacturers, are given below in Table 2.2 for different size detectors. The absolute full energy peak efficiency for a Ge(Li) detector (approximate volume - 50cc) located 25 cm from a point source is given in Fig. 2.16.

TABLE 2.2

TYPICAL Ge(Li) EFFICIENCY AND ENERGY RESOLUTION PARAMETERS FOR ^{60}Co 1.33 MeV GAMMA-RAYS

Nominal Detector Volume (cm^3)	Efficiency Relative to a 3"x 3" NaI Crystal (%)	Peak to Compton Ratio	Energy Resolution FWHM (keV)
20	3 to 4	26:1 to 19:1	3.0 to 2.7
40	7 to 8	30:1 to 24:1	2.1 to 2.7
60	12 to 14	33:1 to 27:1	2.1 to 2.7

From the above, it is obvious that the increases in both the efficiency (relative to NaI) and the peak to Compton ratio that are observed with increasing detector volume reflect the statements made earlier concerning larger detectors.

2.4 New Developments in Germanium Detectors

Improved refining techniques have begun to produce crystals of high purity p or n type germanium (2-5 x 10^{10} impurities/cm^3). Detectors made from this low impurity concentration material are operated in a manner similar to the Ge(Li) detectors described previously, but they are not compensated with lithium during fabrication. (The process of lithium drifting for lower purity germanium is discussed in Section 2.1.) They must be operated at liquid nitrogen temperatures

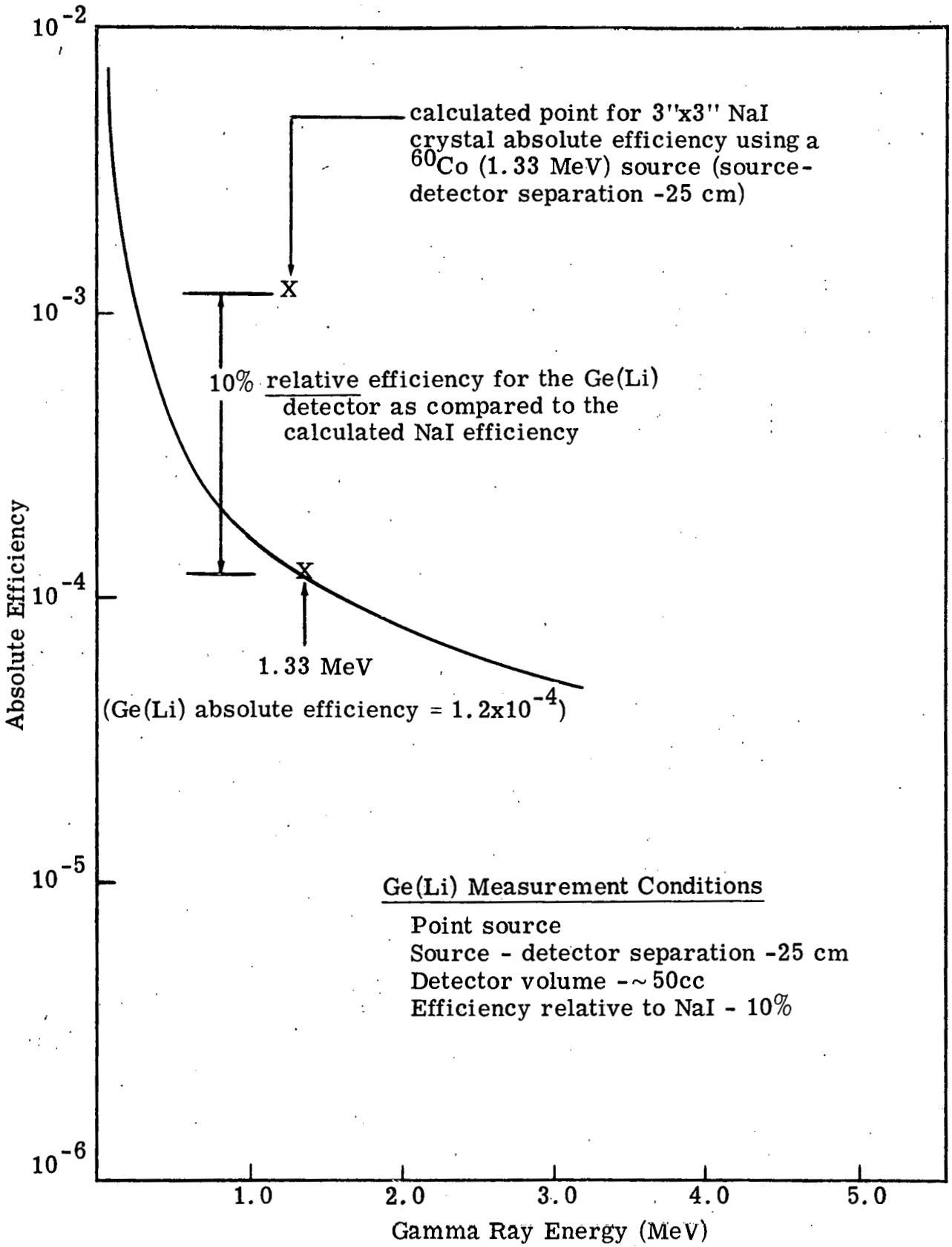

Fig. 2.16. Absolute and relative full energy peak efficiency for a Ge(Li) detector.[36]

to reduce the leakage currents to operating levels when detector bias is applied. However, they do not exhibit an undesirable characteristic of lithium drifted detectors which suffer a change in performance (usually a degradation in resolution) if they are allowed to warm up to room temperature and are then recooled. This change is due to the migration of lithium ions in the crystal at room temperatures. Pure germanium detectors are an attractive possibility for Safeguards applications, since they could be transported at room temperature without bulky dewars and attendant liquid nitrogen replenishment problems. Many high purity devices which are presently in use still require an evacuated container to prevent contamination of the surfaces. However, further development may even eliminate the requirement for an evacuated container when the detector is at room temperature.

Pure germanium detectors are not being fabricated in large volumes at the present time. Typical detectors presently in use have volumes of 1 to 3 cc with energy resolutions and efficiencies comparable to Ge(Li) detectors of the same size. In order to make larger, more efficient detectors, larger samples of material are needed with good crystallography throughout and low, uniform impurity concentrations. These problems do not appear to be insurmountable and pure germanium crystals in the 20 to 40 cc range could be available within several years. These detectors would require cooling only while they are actually in use.

III. A SODIUM IODIDE DETECTOR FOR GAMMA-RAYS

3.1 Theory of Operation

The sodium iodide (NaI) detector for gamma-rays is a scintillation spectrometer, that is, the method of measuring spectra with this device is based on the observation of flashes of light produced by the interaction of gamma rays in a scintillating material. The detector consists of two basic components; a NaI scintillating crystal and an electron photomultiplier tube for converting the small light pulses into measurable electrical signals (Fig. 3.1).

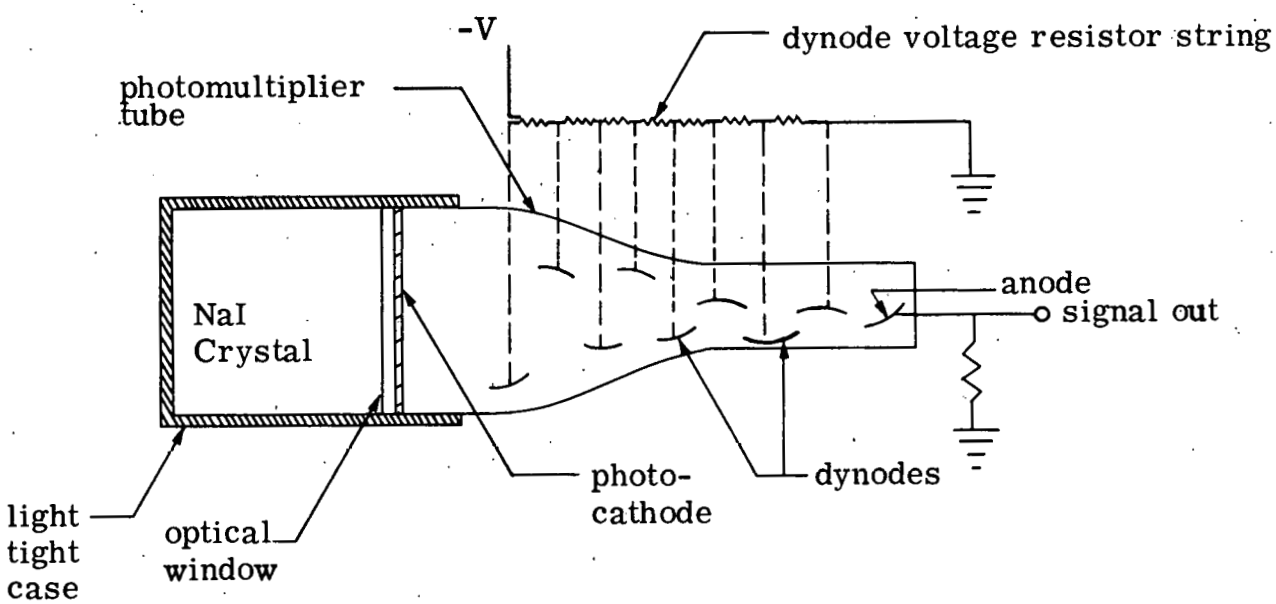

Fig. 3.1. NaI detector.

NaI Crystal

The gamma sensitive volume of the detector consists of a clear crystal of NaI. It is "activated" so that it will scintillate

efficiently by the addition of a small amount of thallium impurity in the crystal lattice (~0.1%). Gamma-rays incident on the detector can interact in the crystal by photoelectric absorption, Compton scattering, pair production* and in combinations of these basic interactions. These processes release free electrons which in turn produce ionization and additional free charge in the crystal. The free charge migrates through the crystal lattice where some is captured at activator sites or trapping centers causing the excitation of the impurity atoms located there. The impurity atoms then de-excite (in times of the order of 10^{-8} seconds) by the emission of light photons with wavelengths on the order of 4100 A^{o}. This process of converting high energy gamma-ray energy into light is illustrated in Fig. 3.2.

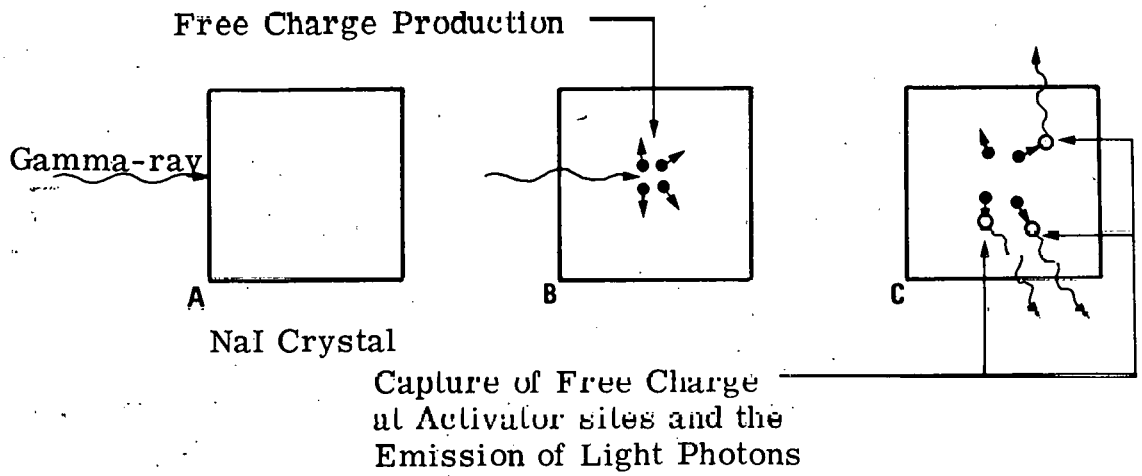

Fig. 3.2 Sequence of events for light production in NaI by gamma-rays.

* The primary interactions of gamma radiation with matter are fundamental and occur in all materials (and detectors). The relative probability with which these interactions occur, however, are dependent on the particular material (or detector). (The basic gamma-ray interactions with matter are described in the previous section on Ge(Li) detectors.)

The average efficiency of converting free electron energy into light photons is approximately 1 photon per 30 to 50 eV of electron energy. Because the basic gamma interactions are identical in NaI and Ge(Li) detectors, the equations given in Section 2.1 can be modified slightly to represent the average number of light photons produced for the various gamma-ray interactions within the crystal. These are given below.

$$n_L = \frac{E_\gamma}{\epsilon_L} \quad \text{(photoelectric absorption and full energy absorption multiple processes)} \tag{3.1}$$

$$n_L = 0 \text{ to } \frac{E_{max}}{\epsilon_L};$$

$$E_{max} = \frac{E_\gamma}{1 + \frac{m_o c^2}{2E_\gamma}} \quad \text{(Compton scattering)} \tag{3.2}$$

$$n_L = \frac{E_\gamma - 1.022 \text{ MeV}}{\epsilon_L} \quad \text{(Pair production-double escape)} \tag{3.3}$$

$$n_L = \frac{E_\gamma - 0.511 \text{ MeV}}{\epsilon_L} \quad \text{(Pair production-single escape)} \tag{3.4}$$

where

n_L = average number of light photons produced for a gamma-ray of energy E_γ(MeV).

ϵ_L = average energy required to produce a light photon (approximately 50 eV).

$m_o c^2$ = electron rest mass (0.511 MeV).

E_γ = incident gamma ray energy (eV).

Photomultiplier Tube

The light pulses produced by the interaction of gamma rays within a NaI crystal are too weak to be seen with the human eye. A device which can detect a very weak pulse of light and convert the light into an amplified electrical signal is the photomultiplier (PM) tube. Moreover, the amplitude of the amplified electrical output pulse is proportional to the intensity of the input light pulse (and hence to the incident gamma ray energy).* Therefore, a measurement of the number of electrical pulses from the PM tube as a function of their size is directly related to the gamma ray spectrum incident on the NaI crystal.

The photomultiplier tube consists of (1) a photocathode which converts the light signal into an electrical signal and (2) a series of dynodes which amplify this electrical signal; the entire structure is contained in a vacuum and resembles a large radio tube. The most frequently used tubes contain a Cs-Sb or Cs-K-Sb photocathode; light photons with wavelengths around 4000 A^{o} incident on this material cause the emission of energetic photoelectrons.

The photoelectrons are electrostatically focused and accelerated onto the first dynode whose surface is coated with a

---

* The relationship is not precisely linear; further information on the deviations from linearity can be found in several of the suggested references on NaI detectors.

secondary emitting material. This material (typically Cs-Sb or Ag-Mg) has the property that when it is bombarded by electrons with energies of several hundred eV, more electrons are emitted from the surface than the number incident on it. Typical values for a dynode multiplication factor fall between 3 and 5.* Electrons from the first dynode are focused onto a second dynode, those from the second onto a third, etc. Thus, by an appropriate arrangement of a series of secondary emitting surfaces, a cascade amplification of the original photocathode current is obtained. The process is illustrated in Fig. 3.3.

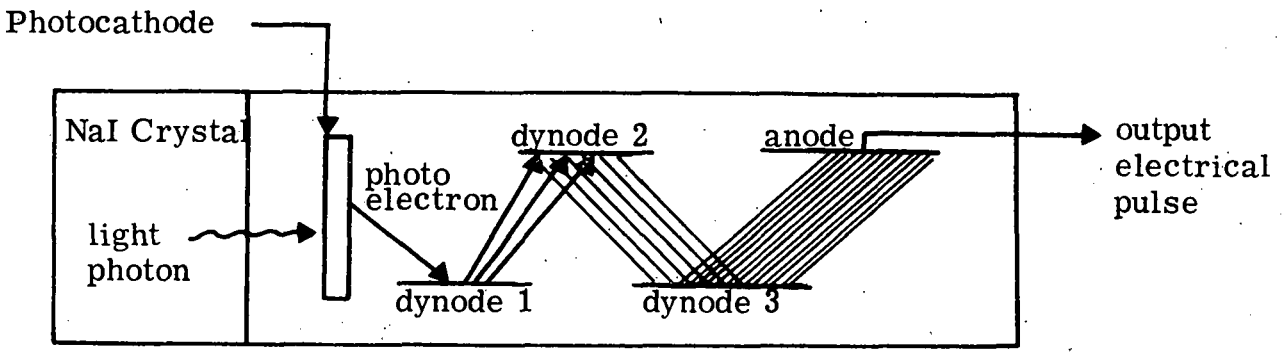

Fig. 3.3. Photomultiplier tube operation

The gain or amplification (G) of the tube is given by:

$$G = \delta^n \qquad (3.5)$$

* dynode multiplication factor = $\frac{\text{number of electrons which leave the surface}}{\text{number of electrons incident on the surface}}$

This factor depends on the dynode material and the voltage applied between dynodes - the values given here are for typical operating conditions.

where

δ = dynode multiplication factor (3 to 5)

n = number of dynodes.

Therefore, a PM tube with 12 dynodes (or stages) and a dynode multiplication factor of 4 has a gain of $(4)^{12}$ or approximately 10^7.

The typical transit time of an electrical pulse through the dynode structure is 20 to 80 nanoseconds. Characteristics for two commercial photomultiplier tubes commonly used with NaI crystals are given in Table 3.1. The cross section of a typical PM tube (type 150 AVP) is shown in Fig. 3.4.

TABLE 3.1
CHARACTERISTICS OF COMMERCIAL PHOTOMULTIPLIER TUBES

Tube Manufacturer	Tube Number	Size		Cathode Material	Wave length of maximum response	Number of dynodes	Gain*	Total Voltage
		Length (in.)	Dia. (in.)					
Amperex	56-AVP	7.5	2.1	Cs-Sb	4200 ± 300Å	14	10^8	2200V
RCA	8576	5.7	2.1	Cs-K-Sb	3850 ± 300Å	12	4×10^6	2000V

*The gain is that which is obtained for the total voltage specified. The total voltage is that applied across the entire string of dynodes.

An idea of the size of the signals generated in a NaI gamma detector system can be obtained from the following example: Assume that a 0.5 MeV gamma ray is totally absorbed in a NaI crystal. The average number of light photons generated (n_L) is (from equation 3.1):

$$n_L = \frac{0.5 \times 10^6 \text{ eV}}{50 \text{ eV/photon}}$$

$$n_L = 1.0 \times 10^4 \text{ photons}$$

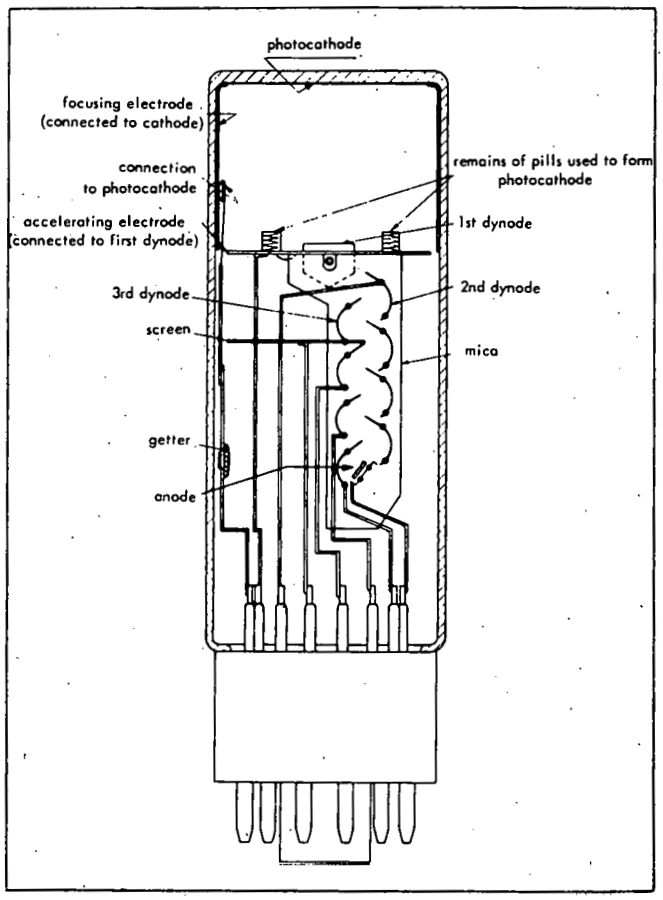

Fig. 3.4. Cross section of a typical photomultiplier tube. (Amperex Electronics Corp. data sheets).

These photons have an average wavelength of 4100 Å (or equivalently, an average energy of about 3 eV). A typical conversion efficiency for a photocathode is about 5×10^{-2} photo electrons/eV of light energy. Therefore, the number of photoelectrons produced at the photocathode (N_p) (assuming all the light is collected) is:

$$N_p = (1.0 \times 10^4 \text{ photons}) (3 \text{ eV/photon}) (5 \times 10^{-2} \text{ photoelectrons/eV})$$

$$N_p = 1.5 \times 10^3 \text{ photoelectrons}$$

Assuming all these photoelectrons are collected at the first dynode and the PM tube has a gain (G) of 10^7, the total charge (N_T) in the pulse which appears at the output is:

$$N_T = N_p G$$
$$= 1.5 \times 10^3 \ (10^7) \ (1.6 \times 10^{-19} \text{ coulombs/electron})$$
$$= 2.4 \times 10^{-9} \text{ coulombs}$$

Since this charge can be collected in times of the order of a microsecond, the signals correspond to peak currents up to about a milliamp. Amplifiers are used to raise this signal level to values which can be conveniently recorded.

If the number of electrical pulses are recorded as a function of their amplitude, spectra such as those shown in Fig. 3.5a and 3.5b are recorded. (Fig. 3.5a is a spectrum from 0.662 MeV incident gamma rays and Fig. 3.5b corresponds to 1.38 and 2.76 MeV incident gamma rays.) As in the case of Ge(Li) detectors, full energy peaks due to photoabsorption and multiple processes are clearly visible for each of the incident gamma-rays. The continuum from Compton scattering is also evident, as are the "Compton edges"

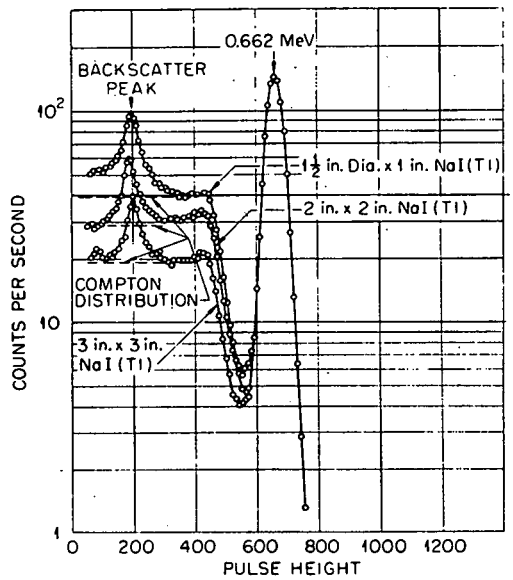

Fig. 3.5a. Comparative responses of several sizes of NaI(Tl) crystals to Cs^{137} gamma-rays.(22)

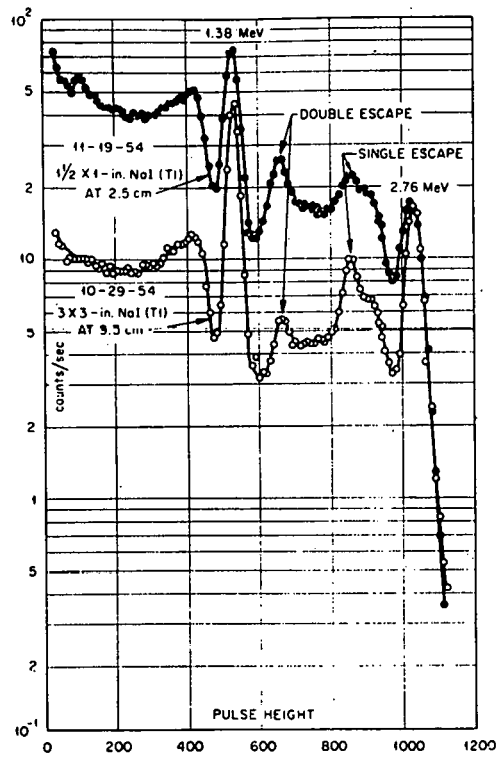

Fig. 3.5b. The response to the two gamma-rays of Na^{24} for 1-1/2 x 1 inch and 3 x 3 inch NaI(Tl) crystals. (22)

(the maximum energy which can be imparted to an electron in a Compton scattering event (E_{max})) at

$$E_{max} = \frac{E_\gamma}{1+\frac{m_o c^2}{2E_\gamma}} \tag{2.3}$$

The events between E_{max} and the full energy peak are due to incident gamma rays which undergo multiple Compton scatterings within the crystal and which finally escape without depositing all their energy in the detector, or which undergo combinations of pair production followed by Compton scattering and escape of the annihilation gammas (Fig. 3.5b). No events related to pair production are evident in Fig. 3.5a because the incident gamma-ray energy is less than the minimum energy required for this process (1.022 MeV). The single and double escape peaks from pair production processes are easily seen for the 2.76 MeV gamma ray in Fig. 3.5b. The peak labeled "backscatter" in Fig. 3.5a is due to gamma rays which scatter from the surroundings into the crystal. The backscatter peak energy corresponds to gamma-rays which have scattered through an angle of about 180^o; analytically,

$$E(\text{backscatter}) = E_\gamma \left(1 - \frac{1}{1+\frac{0.511\ \text{MeV}}{2E_\gamma}}\right) \tag{3.6}$$

From this expression for the backscatter peak energy, it can be determined that the backscatter peak will always be found at an energy less than $\frac{m_o c^2}{2}$ (about 256 KeV), irrespective of the incident gamma ray energy (E_γ) and that the difference between E_γ and E (backscatter) decreases for decreasing incident gamma ray energy.

The effect of using larger detector volumes to increase the ratio of the number of events which appear in the photopeak, compared to the number of events which appear in the continuum can be easily seen in Figs. 3.5a and 3.5b. As in the case of Ge(Li) detectors, this effect is based on the fact that a larger sensitive volume increases the probability for multiple interactions. Therefore Compton scattered gamma rays and annihilation gamma rays following pair production are more likely to be absorbed and the total energy of the incident gamma ray is deposited in the detector.

Therefore, as in the case of Ge(Li) detectors, the use of NaI detectors for Safeguards assays is obvious. The measured gamma ray spectra are characterized by peaks which correspond to the energy and intensity of the gamma rays incident on the detector. Since the energy and intensity of the incident gamma rays depend on the amount and composition of nuclear material in the sample, a measure of the peak's energy and the counts within the peak can be used to assay the sample.

3.2 Description of NaI Detector Systems

NaI gamma ray detector systems contain the following components:

(A) NaI crystal, suitable packaged

(B) Photomultiplier tube

(C) Detector electronics (preamplifier, main amplifier, and pulse height analyzer).

A. NaI Crystal

NaI crystals are available in a variety of shapes and sizes; right circular cylinders up to 6 inches deep and 6 inches in diameter are available commercially as off-the-shelf items. The crystals are hygroscopic so that they must be kept in hermetically sealed containers. Generally, the crystals are surrounded by a thin layer of MgO or Al_2O_3 (a reflecting surface for efficient light collection) and then packed in an aluminum casing. The crystals are relatively fragile, especially the larger sizes, and care should be taken not to subject them to mechanical or thermal shocks to avoid cracking them. The aluminum casing may have an optical window for transmission of the light pulses to the photomultiplier tube, or in some cases the crystal may be mounted permanently to the face of the photomultiplier tube. In either case, good optical coupling between surfaces is obtained by applying a thin layer of a high viscosity silicone oil between them (e.g., Dow Corning DC-200). A typical arrangement is shown in Fig. 3.6. In some special cases, a plastic light pipe may be used to couple the crystal to the PM tube in order to place the scintillator further from the photocathode or to couple a small (large) crystal to a larger (smaller) photocathode area.

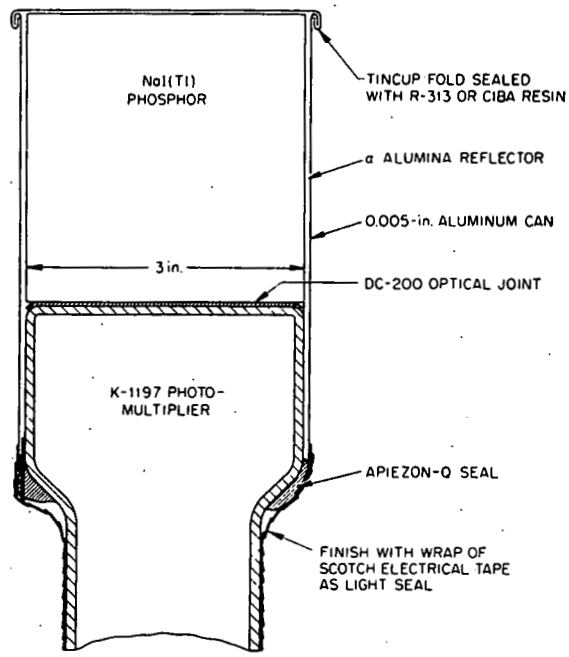

Fig. 3.6. NaI crystal mounted on a PM tube.[22]

B. Photomultiplier Tube

The PM tube resembles a large radio tube. Commonly used tubes have photocathodes ranging from 2 to 5 inches in diameter. There is a set of pins at the bottom of the tube which plug into a tube base which contains the high voltage resistor string for the dynodes and usually a simple preamplifier as well. The entire PM tube is usually surrounded by a magnetic shield of high permeability material such as CO-NETIC and/or NETIC.* The shield prevents the earth's magnetic field and other stray magnetic fields from defocusing the low energy electron trajectories within the tube which would degrade the performance. A typical NaI crystal-PM tube assembly is shown in Fig. 3.7.

C. Detector Electronics

A block diagram of the NaI detector electronics is shown in Fig. 3.8.

---

* Trade names.

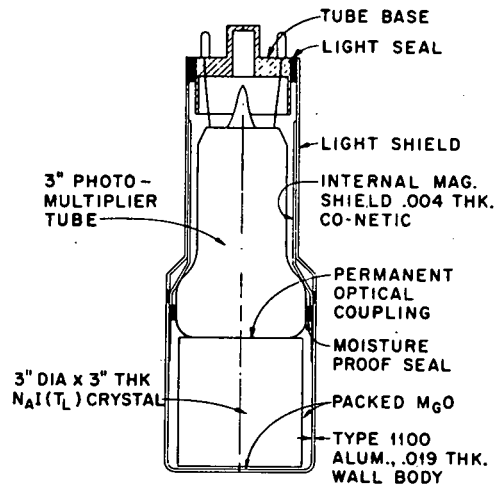

Fig. 3.7. Typical NaI crystal PM tube assembly.(22)

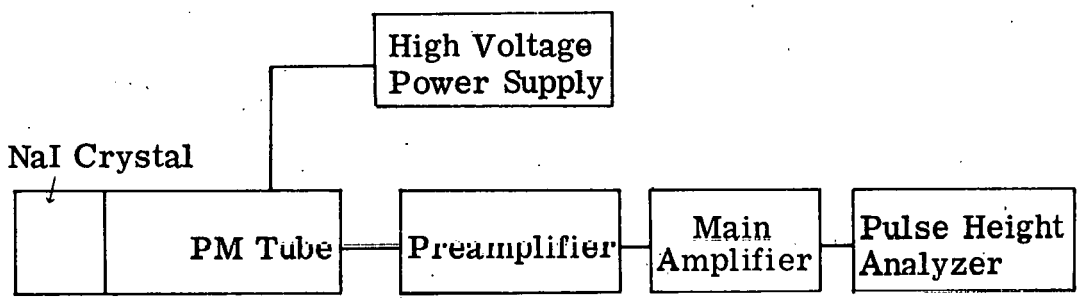

Fig. 3.8. Block diagram for detector electronics.

The electronic components used to make up the NaI detector system are the same as those used in the Ge(Li) system. However, although the components satisfy the same functions as those described in Section 2.2 for Ge(Li) systems, the specifications for the individual

components need not be quite as stringent, since the intrinsic energy resolution of the NaI detector is much poorer than that of a Ge(Li) system. Therefore, electronic problems which would noticeably degrade the energy resolution of the Ge(Li) system, may be undetectable when present in a NaI system. Energy resolution for NaI systems will be covered in greater detail in the following sections.

3.3 Performance Characteristics of NaI Systems

The same characteristics which were used to evaluate Ge(Li) systems for Safeguards nuclear material assay applications are important for evaluating NaI systems. These are:

(A) Energy resolution

(B) Efficiency

As the performance of NaI systems is examined, it will be contrasted with that of Ge(Li) detector systems. This will afford the reader with a chance to directly compare the relative merits of the two alternative systems.

A. Energy Resolution

The energy resolution is parametrized by a measurement of the full width at half maximum (FWHM) of the full energy peak as explained in Section 2.3. Several important factors contribute to the observed width of the peaks in a NaI gamma-ray spectrum:

1. The production of light photons in the NaI crystal by incident gamma-rays is a statistical process so that there is an intrinsic spread in the signal strength due to incident gamma-rays of a given energy. In addition to the statistical effect, local variations in scintillator efficiency and edge effects also contribute to an increased peak width.
2. Imperfections in the process of collecting light photons at the photocathode results in increases in the observed resolution. The effects of self absorption, reflection losses and optical flaws in the coupling between PM tube and crystal all contribute to increases in the observed peak width.
3. The production of photoelectrons in the photocathode of the PM tube which will successfully reach the first dynode is a statistical process and fluctuations here add to the observed NaI peak width. Some PM tubes suitable for gamma-ray spectroscopy have focusing grids between the photocathode and first dynode which can be adjusted to enhance the photoelectron collection and hence reduce the importance of this effect. Nonuniformity of the

photocathode response also adds to the broadening of the observed peak width.

4. Finally, the amplification of the electrical signal in the dynode structure is also a statistical process which adds to the peak width. (This is based on the fact that secondary emission is a statistical phenomenon.) The effect is especially important at the first dynode where the number of incident electrons is small and statistical fluctuations are therefore large. For this reason, the first dynode may have a higher voltage drop and be constructed of a material with an especially high secondary emission ratio. The importance of this effect can be reduced by raising the dynode-to-dynode voltage up to the point where further increases in amplification result in thermal noise problems, or non-linear responses are observed. The addition to the system resolution due to amplification of the photocathode signal varies as E_γ^{-1}.

The total NaI system resolution is sometimes expressed as follows:

$$R = \sqrt{A^2 + B^2} \tag{3.7}$$

where

R = NaI system resolution (percent)

A, B = contributions to the system resolution due to:

(A) light production and collection

(B) photoelectron production and collection at the first dynode and PM tube amplification.

These quantities are given in Table 3.2 as measured for a given crystal-PM tube combination at several gamma ray energies.

TABLE 3.2

ENERGY RESOLUTION COMPONENTS FOR A NaI DETECTOR [24]

E_γ(MeV)	R(%)	A(%)	(B%)
0.21	10.9	8.3	7.1
0.66	7.7	6.6	4.0
1.07	6.6	5.8	3.2

The energy resolution for a NaI detector system is often quoted for the 0.662 MeV gamma rays from ^{137}Cs. Typical figures range from 7.5 to 13.0% depending on the particular detector configuration. Resolutions as low as 7.0% have been reported for specially designed systems. In comparison, Ge(Li) systems have energy resolutions on the order of 0.4 to 0.6% under the same conditions. This is about 20 times better than the NaI system; the fact is graphically illustrated in Fig. 3.9.

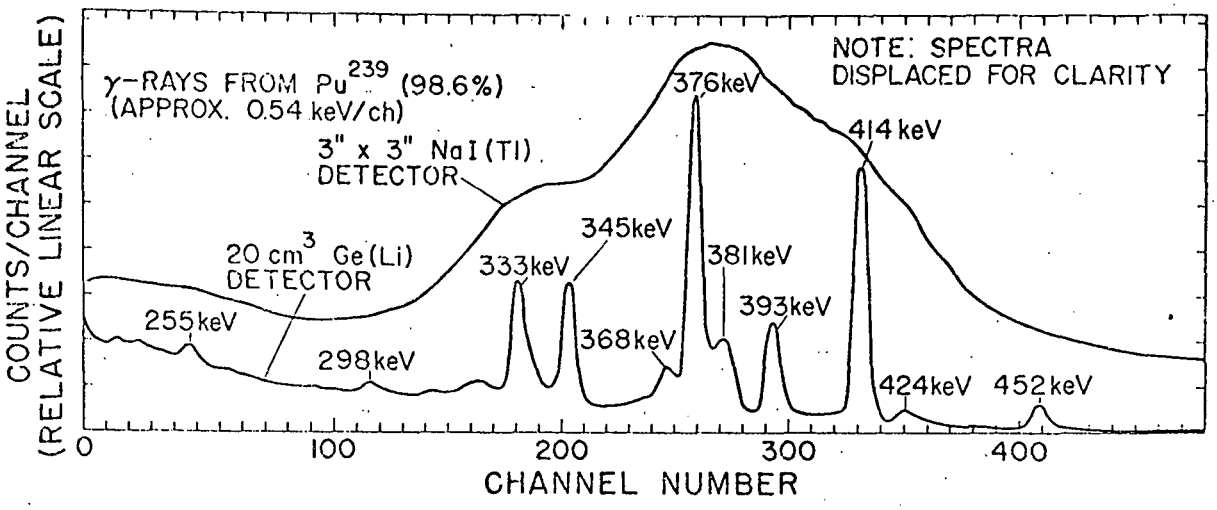

Fig. 3.9. Comparison of NaI and Ge(Li) resolutions for the same gamma-rays.[21]

Due to the significantly poorer resolution obtained from NaI systems, noise problems introduced by presently available nuclear preamplifiers and amplifiers are relatively insignificant; although excessive count rates and carelessly tuned amplifiers can still broaden the resolution to figures higher than those quoted above. Because of the inherently poorer resolution, Safeguards assay problems which are adequately handled by NaI detectors may successfully employ pulse height analyzers with a limited number of channels or even single channel analyzers to store and display the data.

It is evident that for assay samples where it is necessary to separate peaks which lie close together, the high resolution Ge(Li) detector is the most appropriate system to use. An illustration of this is shown in Fig. 3.10 where the resolution of the 203.5 and 207.9 KeV

peaks in a spectrum taken from a plutonium sample provide a useful means of measuring the $^{241}Pu/^{239}Pu$ ratio. A NaI spectrum from the same sample would never show these two gamma ray lines as separate peaks.

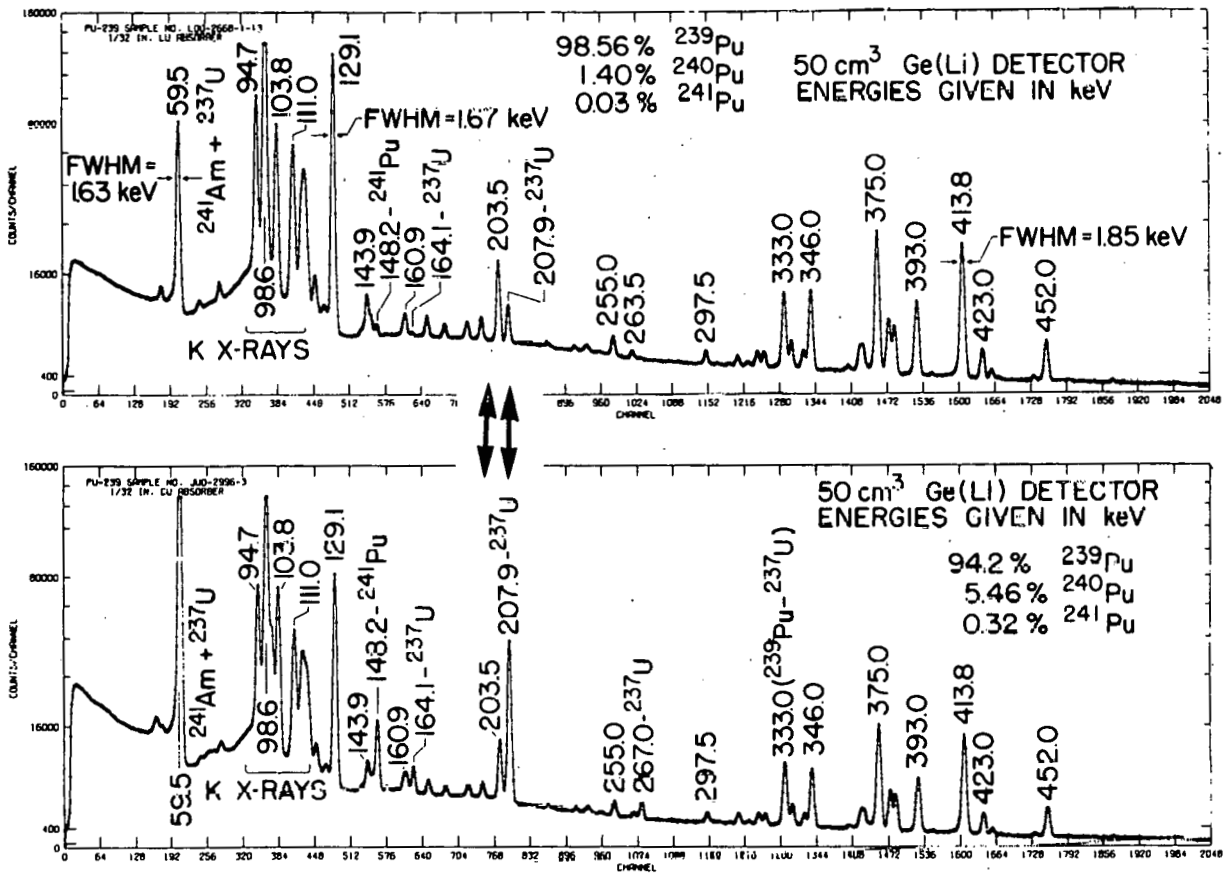

Fig. 3.10. Gamma-ray spectra of two different isotopic compositions of plutonium as measured with a high resolution 50 cm^3 Ge(Li) detector. The heavy arrows indicate position of the ^{239}Pu-^{241}Pu "doublet" which provides a useful isotopic ratio measurement, independent of gamma attenuation.[21]

Detector Efficiency

It was pointed out in Section 2 that larger detectors imply greater detection efficiency due to increased solid angle, longer path lengths of the incident radiation through the detector, and increased probability for multiple processes to occur. Larger detectors thus add events to the useful information contained in the full energy peak. This is illustrated by the gamma spectra shown in Figs. 3.5a and 3.5b for NaI crystals of different sizes.

The total peak efficiency versus incident gamma ray energy for a 3-inch diameter x 3 inch deep NaI crystal located 20 centimeters from the assay sample is given in Fig. 3.11. At 1.3 MeV, the peak efficiency is about 20%; i.e., 20% of the gamma rays incident on the detector will be detected and appear in the full energy peak. Ge(Li) detectors with a volume of 40 cm^3 have an efficiency of about 7% of that of the NaI; i.e., about 0.07 x 20% or 1.4% of the gamma rays incident on a 40 cm^3 Ge(Li) detector will be detected and appear in the full energy peak. The largest and most efficient Ge(Li) detectors produced today cannot do much more than triple this figure, hence one concludes that NaI detectors are approximately 5 to 10 times more efficient than their Ge(Li) counterparts.

This, however, does not give a complete picture of the actual situation. Figure 3.12 shows the peak to total ratio for several NaI

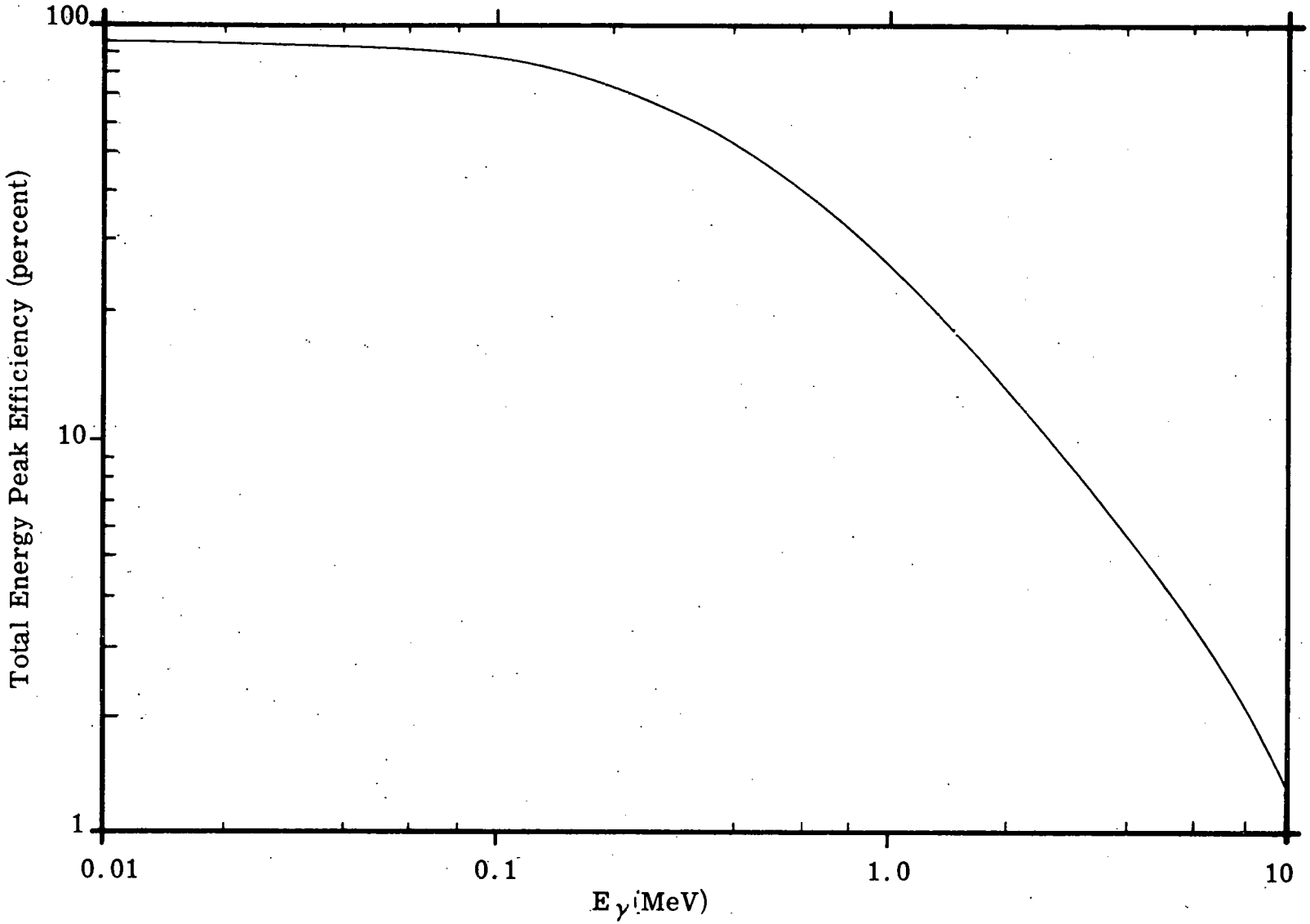

Fig. 3.11. Total energy peak efficiency vs. gamma ray energy for a 3" x 3" NaI-20 cm from sample.

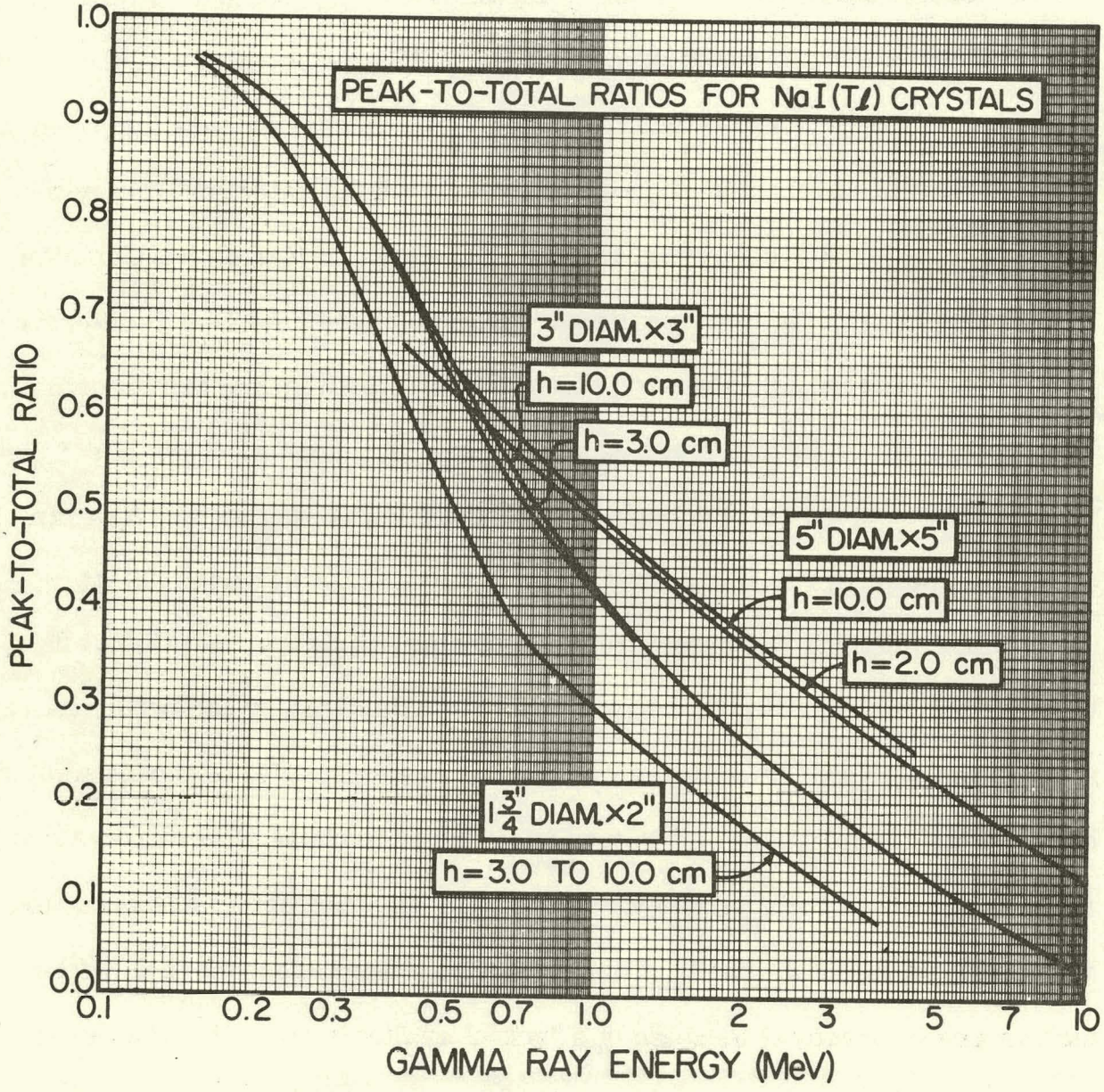

Figure 3.12. Peak to total ratios for NaI crystals (h is the sample to detector separation).[4]

crystals. This parameter is defined as the fraction of counts which will appear in the total energy peak compared to the total number of counts detected. From this figure it is evident that a sizeable fraction of the events recorded will appear in the Compton scattering continuum (e.g., at 1.3 MeV and a sample-detector separation of 10 cm, about 65% of the events recorded will be in the continuum). Therefore, in cases where a number of gamma-rays of different energies are incident on the detector, it may be difficult to pick out a low intensity gamma peak which lies atop a Compton background from higher energy lines. In some cases, the Ge(Li) detector with lower efficiency (hence poor statistics) still provides better information by crowding fewer counts into a small number of channels. This effect can create a much more recognizable peak in the gamma spectrum. An example of this is shown in Fig. 3.13 for the ^{238}U peaks at 0.767 and 1.001 MeV.

In summary, NaI detectors have greater efficiency than Ge(Li) detectors, but this is offset in many Safeguards situations by the better energy resolution which can be obtained with Ge(Li) systems. NaI is most useful in cases where the additional efficiency is required because of very low count rates and there is little or no chance of impurities confusing interpretation of the data which is obtained. There are also a few cases where Ge(Li) detectors are impractical because of a lack of available space for the dewar, the absence of liquid nitrogen for cooling, or an inability to provide even the minimal amount of maintainence (liquid nitrogen replenishment) which these detectors require. Even these problems may not be unsolvable, since development still continues in the areas of improved cryogenic systems and more versatile detectors (e.g. the pure germanium crystals).

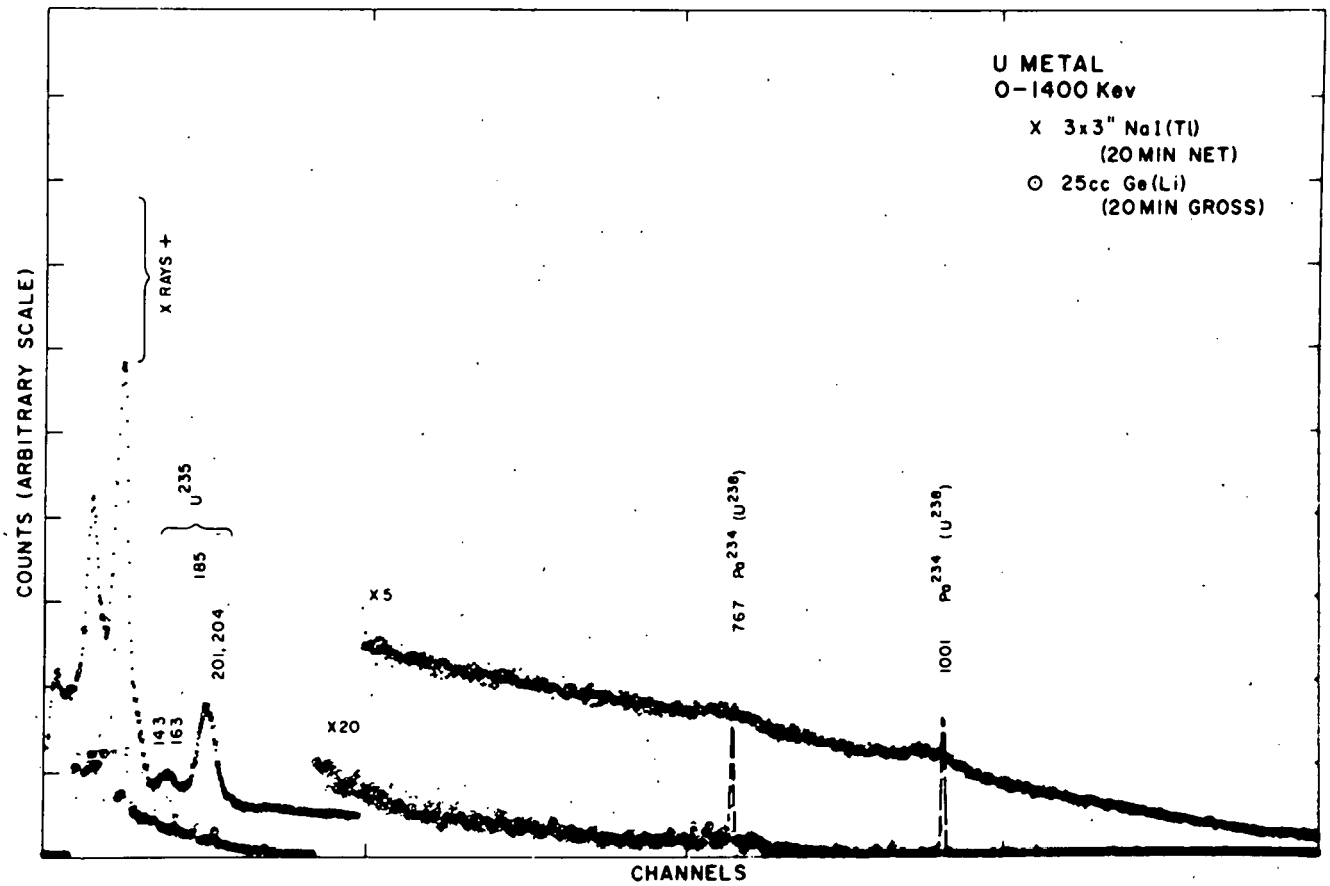

Figure 3.13. NaI and Ge(Li) Spectra from a ^{238}U Sample.[19]

4. AN EXAMPLE OF A NUCLEAR MATERIAL ASSAY USING GAMMA-RAY SPECTROSCOPY

The last section of this document describes a plutonium assay of reactor fuel pins as an example of the use of gamma ray spectroscopy in Safeguards' applications. A relatively simple assay problem was chosen for this example in order to focus attention on the important properties of Ge(Li) and NaI gamma ray detectors that were discussed in the preceding sections. The example is also intended to illustrate the basic procedure for acquiring and processing gamma spectroscopic information for nuclear materials assay work, uncomplicated by considerations imposed by samples with difficult geometries, inhomogeneous distributions of material, and containing non-nuclear matrices of unknown composition. Techniques for dealing with samples which are inherently more difficult to assay are described in the technical literature.

4.1 Sample Description

The nuclear material samples were zero-power-reactor (ZPR) fuel pins. There are three classifications of pins labeled F, G, and H, each containing different loadings of plutonium-uranium oxides. Nominal characteristics for the fuel pins are given in Table 4.1.

TABLE 4.1

ZPR MIXED OXIDE FUEL PIN CHARACTERISTICS

Nominal dimensions - 3/8 in. dia., 6 in. length

Nominal weight - 90g

Cladding - stainless steel

Composition - PuO_2 and UO_2

Classification	w/o Pu	Pu isotopic (%)					
		238	239	240	241	242	^{241}Am
F	13.32	.046	86.72	11.50	1.55	.188	.034
G	26.63	.046	86.53	11.57	1.67	.192	.068
H	15.77	.087	68.45	25.56	4.53	1.38	.061

4.2 Apparatus Description

The fuel pins were assayed in two different setups, one employing a Ge(Li) detector and the other a NaI detector. The measurement geometries and detector characteristics for both setups are shown in Fig. 4.1. The distance between the fuel pin and detector have been adjusted in both cases to keep the analyzer dead time* between 3 and 5 percent. This was done to prevent high counting rates from degrading the system's energy resolution.

*Dead time - the percentage of the total time that the multichannel analyzer cannot accept input signals from the detector because it is "busy" processing information. The multichannel analyzer used automatically corrected the data for dead time, by counting in real time for a period equal in length to the preset count time plus the measured dead time.

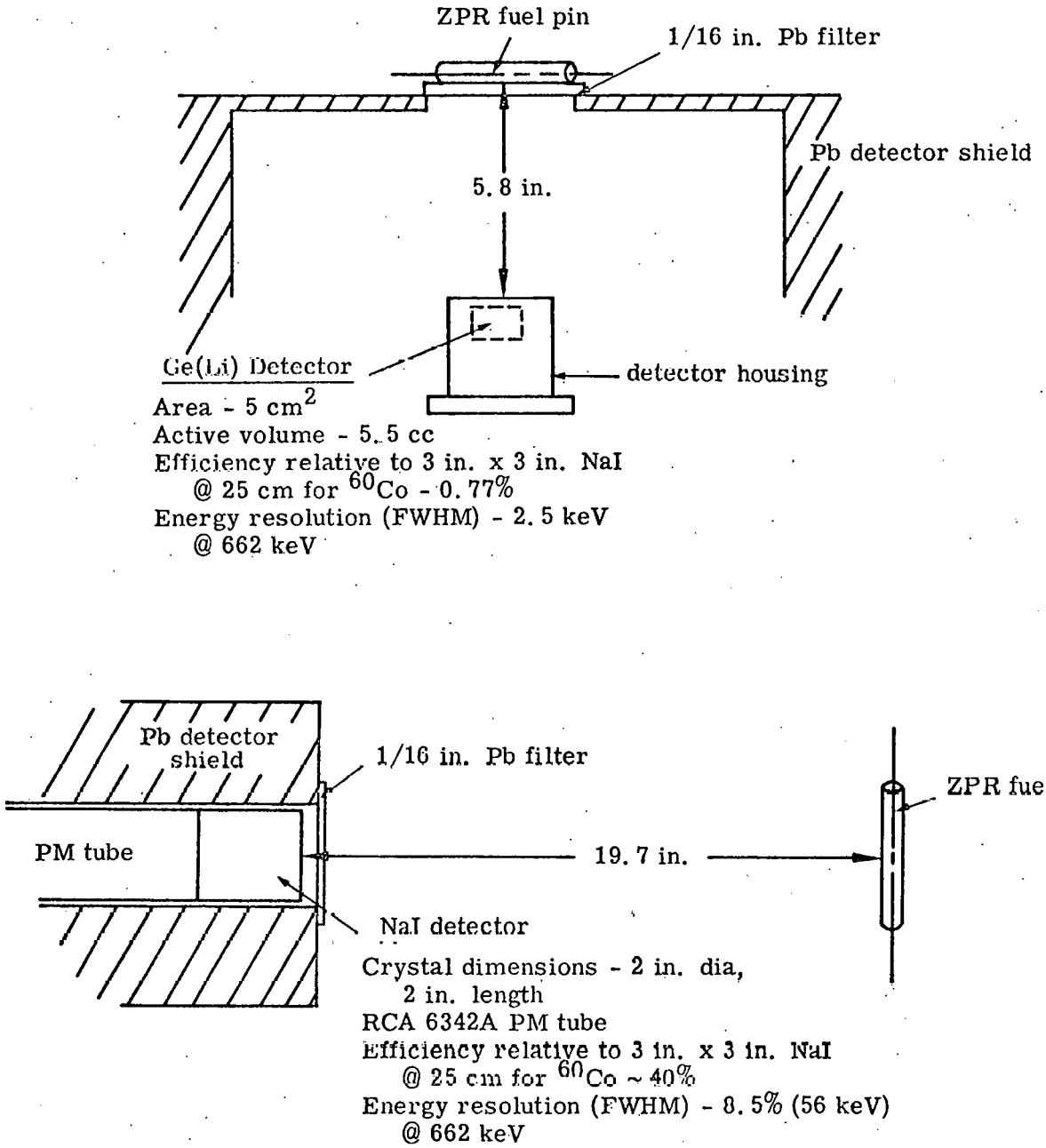

Fig. 4.1. Assay geometries and detector characteristics (Ge(Li) and NaI systems). Not drawn to scale.

The smaller separation between detector and fuel pin in the Ge(Li) setup reflects the fact that the intrinsic gamma ray detection efficiency of the Ge(Li) detector is only several percent of that of the NaI detector. A layer of lead 1/16 in. thick was placed between the detector and fuel pin in both setups to reduce the intensity of the low energy plutonium and uranium X-rays compared to that of the prominent ^{239}Pu 414 KeV gamma ray of interest. (Sixty-eight percent of the 414 KeV gamma rays pass through the 1/16 in. lead filter while less than .01 percent of the plutonium and uranium k X-rays get through). This filter was not optimized for this problem, but it was adequate.

4.3 Analyzer Energy Calibration-Energy Resolution-Sample Identification

It has been previously pointed out that gamma ray spectroscopy can be applied to samples of nuclear materials to identify their contents and to quantify the amount of material present. The first function, that of identification of materials, is accomplished by determining the energy of observable peaks in the spectrum and comparing the results with existing data on gamma ray spectra from standard samples.[11] In order to determine the energy of a peak observed in the multichannel analyzer spectrum, the analyzer must be calibrated with a set of standard radioactive sources. There are a number of such sources available, but for this example, those listed in Table 4.2 were used.

TABLE 4.2

RADIOACTIVE CALIBRATION SOURCES

Radioisotope	Gamma Ray Energy (KeV)
^{137}Cs	661.6
^{22}Na	511.0 1277 (off scale)
^{235}U	185.7 (prominent) and numerous others

The calibration sources were alternately placed in approximately the same position as the fuel rods, but with the 1/16 in. lead filter removed, and counted for 200 seconds. The amplifier gain controls were adjusted so that the ^{137}Cs peak (661.6 KeV) appeared in the upper portion of the 1024 channel spectrum. This insures that the prominent 414 KeV line from ^{239}Pu will be on scale. For purposes of demonstration, the amplifier gain controls on both the Ge(Li) and NaI systems were adjusted so as to position the ^{137}Cs peak in approximately the same channel. The spectra from the three calibration sources are shown for the Ge(Li) and NaI systems in Figs. 4.2 and 4.3 respectively. The following data was then obtained from these spectra for the Ge(Li) system; a similar analysis can be performed for the NaI system.

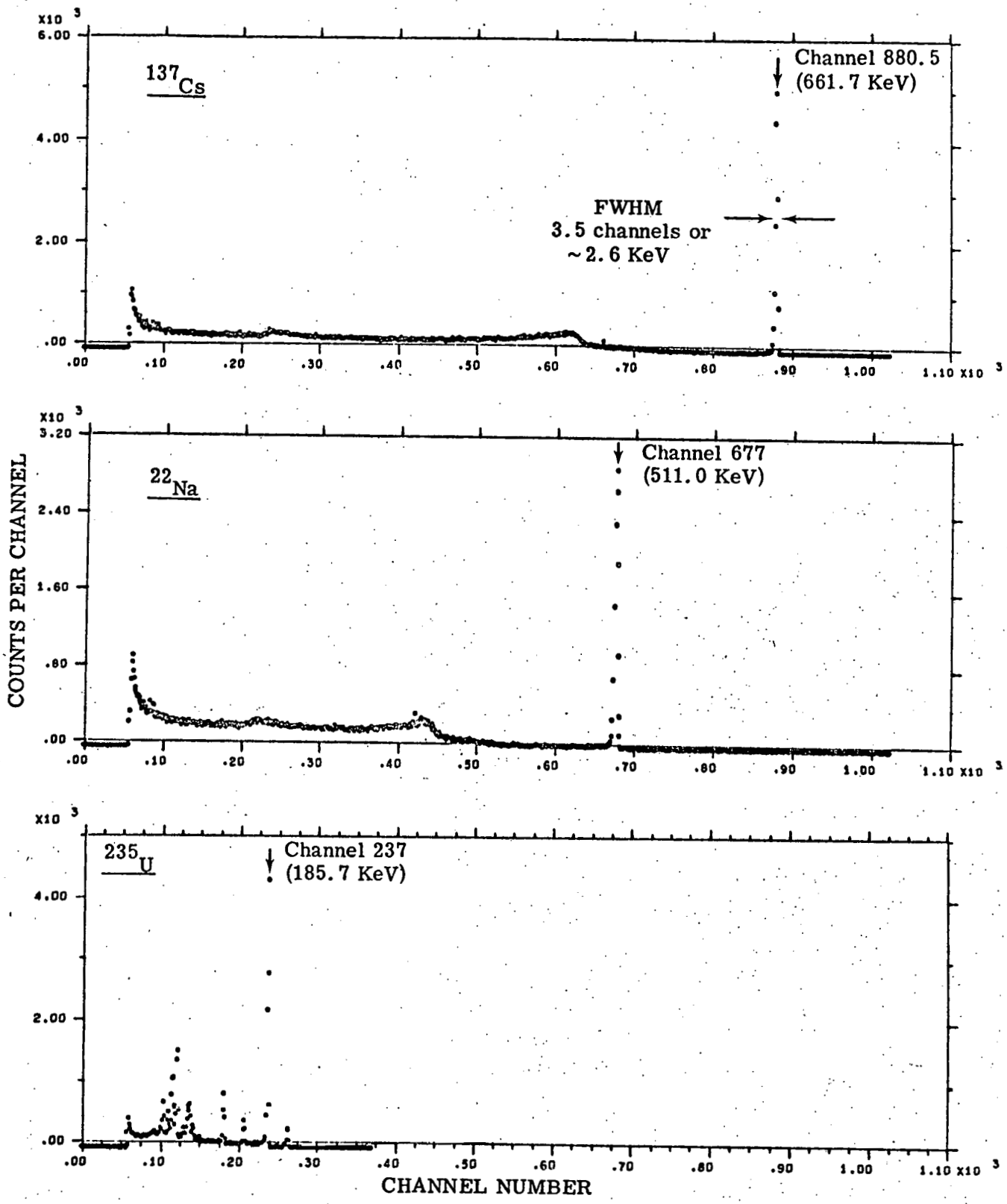

Fig. 4.2. Gc(Li) spectra - energy calibration sources.

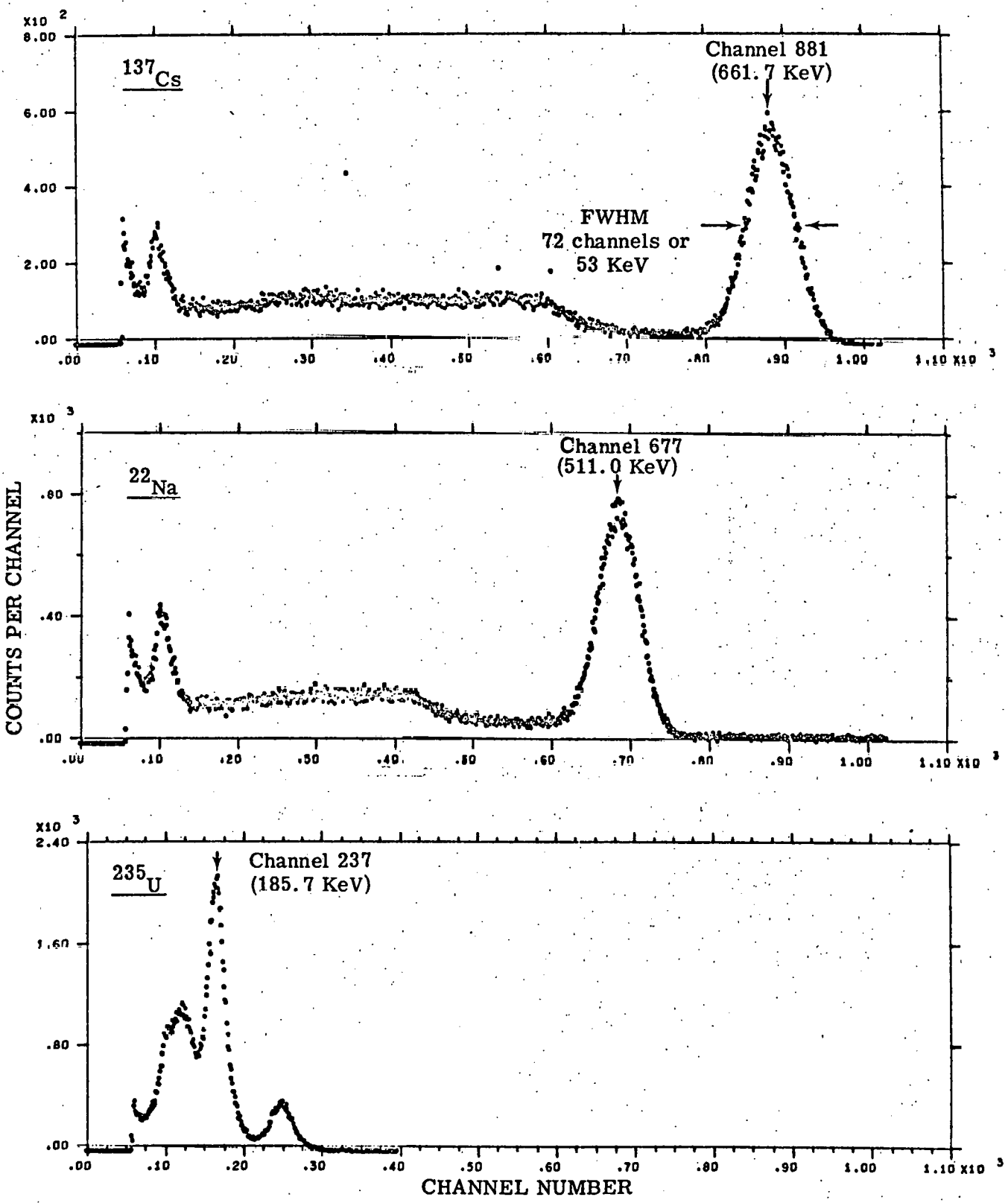

Fig. 4.3. NaI spectra - energy calibration sources.

Calibration Source	Peak Energy (KeV)	Channel Number
^{137}Cs	661.7	880.5
^{22}Na	511.9	677
^{235}U	185.7	237

These data are plotted in Fig. 4.4. A straight line fitted to the measured points shows that the full energy peak of a gamma ray with energy (E_γ) is related to the channel (C) in which it appears by the expression:

$$C(\text{channel no.}) = E_\gamma \text{ (KeV)} \times 1.352 - 13.5 \qquad (4.1)$$

Notice that there is a slight "zero offset", i.e. zero gamma ray energy does not fall in channel zero, but 13.5 channels offscale to the left. This is not important for our calibration, however there is a zero level adjustment on most analyzers which can be used to adjust the calibration so that zero energy does fall in channel zero. Note also that the energy width of each channel is given by:

$$\frac{\Delta E}{\text{channel}} = \frac{1}{1.352}$$

$$\cong 0.74 \text{ KeV/channel}$$

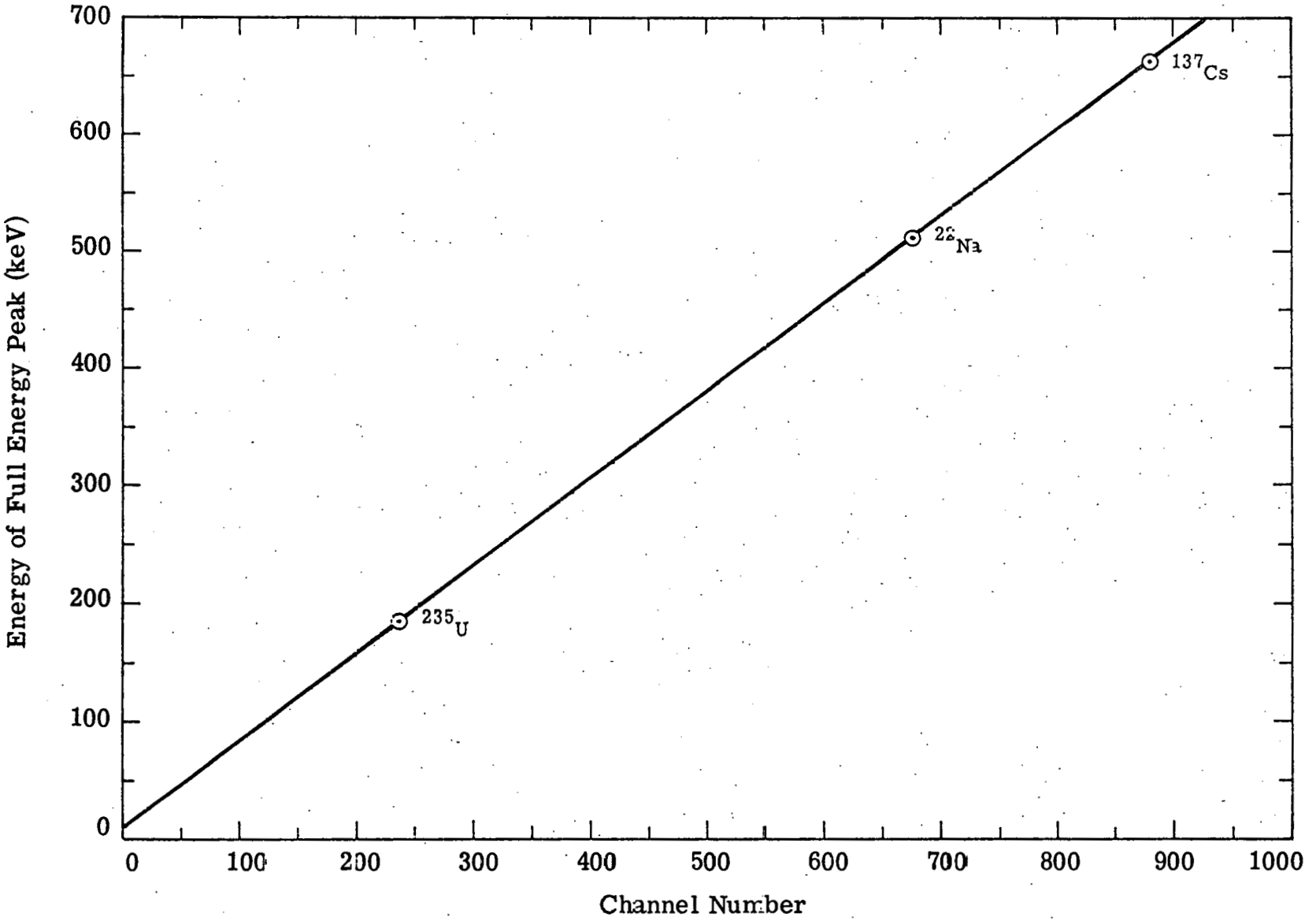

Fig. 4.4. Energy calibration curve (Ge(Li)).

The energy resolution of the ^{137}Cs peak for both detectors can also be measured from the calibration spectra. The full width at half maximum (FWHM) for the Ge(Li) and NaI spectra are approximately 3 and 72 channels respectively.

Ge(Li) (FWHM) = 3 channels x 0.74 KeV/channel = 2.2 KeV

NaI (FWHM) = 72 channels x 0.74 KeV/channel = 53 KeV

or as commonly expressed for NaI, $\frac{53 \text{ KeV}}{662 \text{ KeV}} \simeq 8\%$

After calibration, a fuel pin was placed in position and counted for 1000 seconds in the Ge(Li) setup and for 400 seconds in the NaI setup. The spectra are shown in Fig. 4.5. The Ge(Li) detector shows prominent peaks in the channels listed in Table 4.3, the respective energies can be determined from Fig. 4.4 or from equation 4.1.

The 414 and 375 KeV peaks can be positively identified as originating from ^{239}Pu in the sample; the 332 KeV peak contains counts from ^{239}Pu, however ^{241}Am or ^{237}U could also contribute to the area under the observed peak since the energy resolution of the system is not adequate to separate the different peaks from the individual isotopes. ^{241}Am and ^{237}U (both decay products of ^{241}Pu) are also possible contributors to the 208 KeV peak along with ^{233}U. However, inspection of the spectrum reveals no strong ^{233}U peak at 317.15 KeV[11], so that one can rule out the presence of ^{233}U in the sample, leaving only ^{241}Am and ^{237}U. This cursory comparison of the spectrum with available data has therefore identified presence of ^{239}Pu and possibly ^{241}Pu (through its decay products ^{241}Am

TABLE 4.3

IDENTIFICATION OF PROMINENT PEAKS IN THE FUEL ROD SPECTRA

Channel Number	Energy (KeV) (from Fig. 4.4)	Isotope[11]	Gamma Ray[11] Energy
546	414	^{239}Pu	413.71
493.5	375	^{239}Pu	375.04
435.5	332	^{237}U (^{241}Pu)	332.34
		^{241}Am (^{241}Pu)	332.39
		^{239}Pu	332.84
267.5	208	^{241}Am (^{241}Pu)	208.00
		^{237}U (^{241}Pu)	208.00
		^{233}U	208.18

and ^{237}U) in the sample. Closer inspection of weaker lines in the spectrum coupled with arguments similar to the above can lead to identification of the other plutonium isotopes and ^{238}U as well. Only the stronger lines were considered here to illustrate the technique of material identification. In continuing with this example, we will concentrate our attention on the ^{239}Pu peak at 414 KeV which is uncontaminated by contributions from other isotop

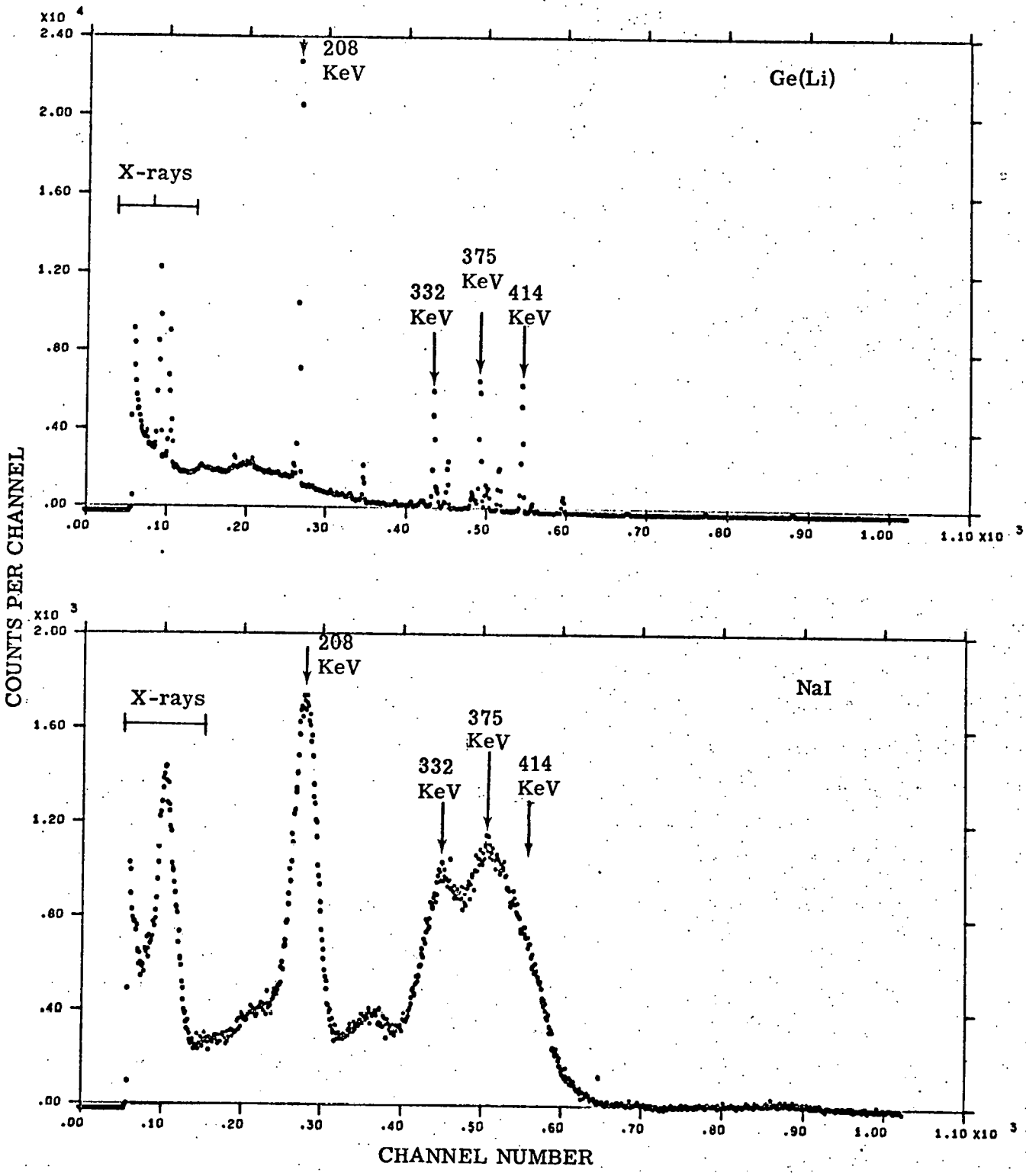

Fig. 4.5. ZPR fuel pin spectra (Ge(Li) and NaI). Prominent peaks are labeled.

It is appropriate at this point to compare the Ge(Li) and NaI spectra from the same ZPR fuel rod. The large Ge(Li) peaks at 414, 375, and 332 KeV (together with a number of smaller peaks) appear as a broad, double humped peak in the NaI spectrum (Fig. 4.5); the large 208 KeV peak is fairly well defined in both spectra. It is obvious from comparison of the respective spectra that some material identification is possible with the poorer resolution NaI system, but that the Ge(Li) spectra offer much more positive information.

Once it has been decided to assay for a particular material, it is often convenient to expand the analyzer presentation over that region of the spectrum where the peaks of interest appear. This can be done by any of several methods including using an analyzer digital offset or using a biased amplifier after the main amplifier. All of these techniques allow the operator to move the zero channel of the spectrum to a selected energy E_L. The spectrum above E_L is then expanded to cover the region of interest from E_L to E_H. This technique is illustrated in Fig. 4.6 (the analyzer digital offset was used in this case). This technique is especially useful where interfering peaks lie close to those of interest, but whereby using a small energy interval per channel, the two can be adequately resolved.

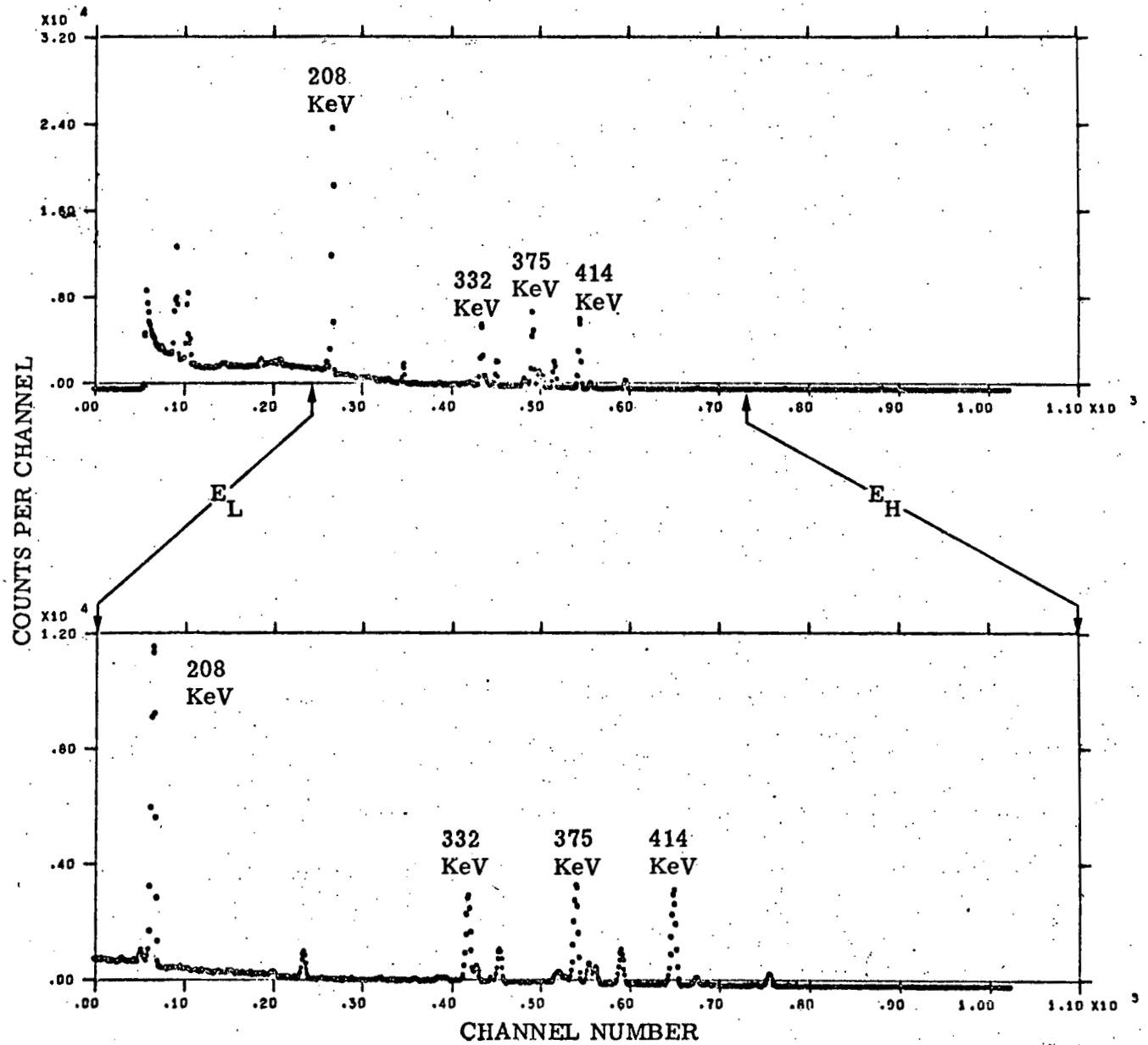

Fig. 4.6. ZPR fuel pin spectra - expanded scale.

4.4 Quantitative Ge(Li) Assay

The technique employed for ^{239}Pu assay of the ZPR fuel pins was to use two fuel pins as known standards and compare the unknown pins with the standard pins. Under normal circumstances, the standards would be carefully sampled and analyzed using destructive or other techniques and the assumptions of homogeneity would be checked. The fuel pins were placed in a reproducible position with respect to the detector and the number of ^{239}Pu 414 KeV gamma rays which interacted in the Ge(Li) detector and appeared in the full energy peak were related to the amount of ^{239}Pu in the sample. This type of assay assumes that the attenuation of gamma rays in the fuel pin cladding is approximately the same for all pins, that the distribution of material in the pins is homogeneous, and that the average atomic number and density of the pin contents is the same for all pins. If for some reason these assumptions were not considered acceptable, other more complicated methods could be used which would eliminate one or more of these assumptions in order to insure an accurate assay. (For example, the pins could be spacially scanned by a collimated detector to detect non-homogeneous distributions of material.)

In this example, two fuel pins were used as standards and the contents of these pins were assumed to be well established. The characteristics of these pins are shown in Table 4.4.

TABLE 4.4

STANDARD ZPR FUEL PINS

Pin Number	Core Weight (g)	w/o Pu	Isotope Percentages						
			238	239	240	241	242	^{241}Am	^{239}Pu Content g
STD 1	89.24	15.767	.0872	68.449	25.556	4.526	1.381	.0607	9.631
STD 2	89.92	26.631	.0460	86.527	11.570	1.665	0.192	.0683	20.72

The basic assay procedure was to place the fuel pin in the position shown in Fig. 4.1. The analyzer was first zeroed and then a count was taken for 1000 seconds (live time) or about 1020 seconds in actual clock time, which corresponds to a dead time of about 2 percent. After the counting period, the spectrum (STD 2) shown in Fig. 4.5 was obtained and the data printed out on paper tape (counts per channel). An expanded view of the 414 KeV region is shown in Fig. 4.7.

The method used for determining the number of counts in the 414 KeV peak shown in Fig. 4.7 is described below: The 414 KeV peak was assumed to lie in channels 541 to 549 (inclusive). The Compton background under the peak was assumed to be that lying below a sloping line drawn under the peak passing through a value in channel 541 equal to the average number of counts/channel in channels 536 to 540 (inclusive) and passing through a value in channel 549

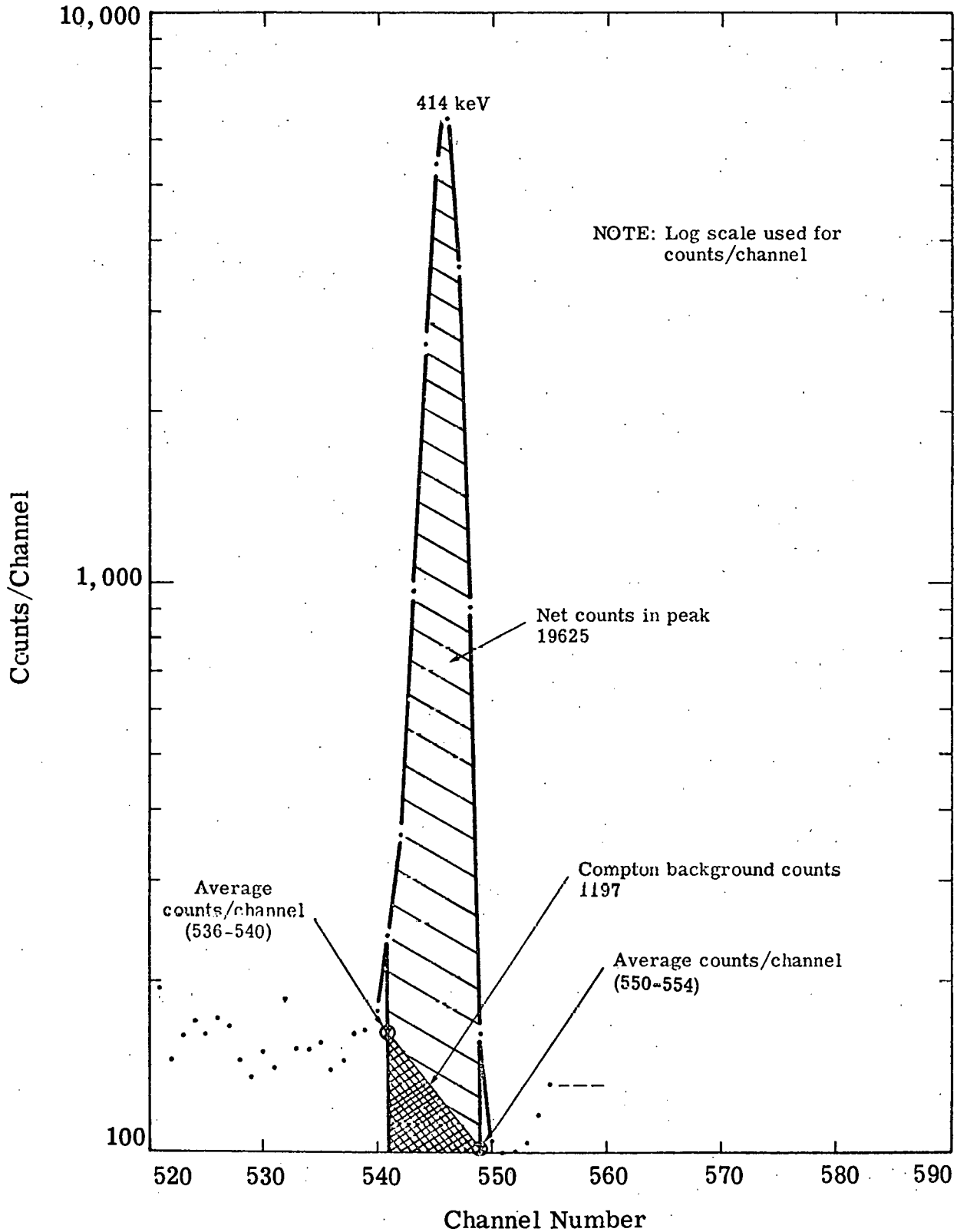

Fig. 4.7. Data reduction - ^{239}Pu 414 keV peak.

equal to the average number of counts/channel in channels 550 to 554 (inclusive). The mathematical expression is given by:

$$\text{Compton background} = \frac{\text{Avg. counts/ch (536-540)} + \text{Avg. counts/ch (550-554)}}{2} \times 9 \text{ ch.} \quad (4.2)$$

Therefore from Fig. 4.7,

Total counts (ch. 541-549 inclusive)	20822	
Average counts/channel (536-540 inclusive)	804/5	= 161
Average counts/channel (550-554 inclusive)	510/5	= 102
Compton background (Eqn. 4.2)	$\frac{161+102}{2} \times 9$	= 1197

Net counts (414 KeV peak) = Total counts - Compton background

= 20822 - 1197

= 19625

The statistical uncertainty (1 standard deviation) of this number is given by:*

$$\text{Statistical standard deviation} = \sqrt{\text{Total Counts} + \text{Compton Background}}$$

$$= \sqrt{20822 + 1197}$$

$$= \sqrt{22019}$$

$$= 148$$

Therefore, assuming the error in the known ^{239}Pu content of STD 2 is negligible:

$$19625 \pm 148 \text{ counts/1000 seconds} = 20.72 \text{ g } ^{239}Pu$$

*See for example, E. Segre, Nuclear and Particles, W. A. Benjamin, Inc. New York (1965).

A similar measurement of STD 1 yields the following result.

$$9126 \pm 104 \text{ counts/1000 sec.} = 9.631\text{g } ^{239}\text{Pu}$$

A straight line relationship between counts versus grams ^{239}Pu was assumed resulting in the calibration chart shown in Fig. 4.8. This relationship between counts versus grams ^{239}Pu can be mathematically expressed as

$$\text{grams } ^{239}\text{Pu} = \frac{\text{counts/1000 sec. (414 KeV peak)}}{946.71} \qquad (4.3)$$

An unknown ZPR fuel pin was placed in the same position as the standards, counted for 1000 seconds and the data was reduced in exactly the same manner described above. The result was 9700 ± 107 counts/1000 seconds. Using Equation 4.3 or Fig. 4.8 and ignoring uncertainties in the calibration curve itself, this result corresponds to $10.25 \pm 0.11\text{g } ^{239}\text{Pu}$. (This is in agreement with the manufacturers value of $10.31\text{g } ^{239}\text{Pu}$.) The unknown result is also plotted on Fig. 4.8.

This completes the presentation of an example of a simple assay problem using gamma spectroscopy. The details of the techniques used to assay the samples and process the data (including the method of background subtraction) are not unique; however, it is most important that the techniques selected be followed consistently for all assays of a given type of sample. It is also appropriate to reemphasize that the underlying basic

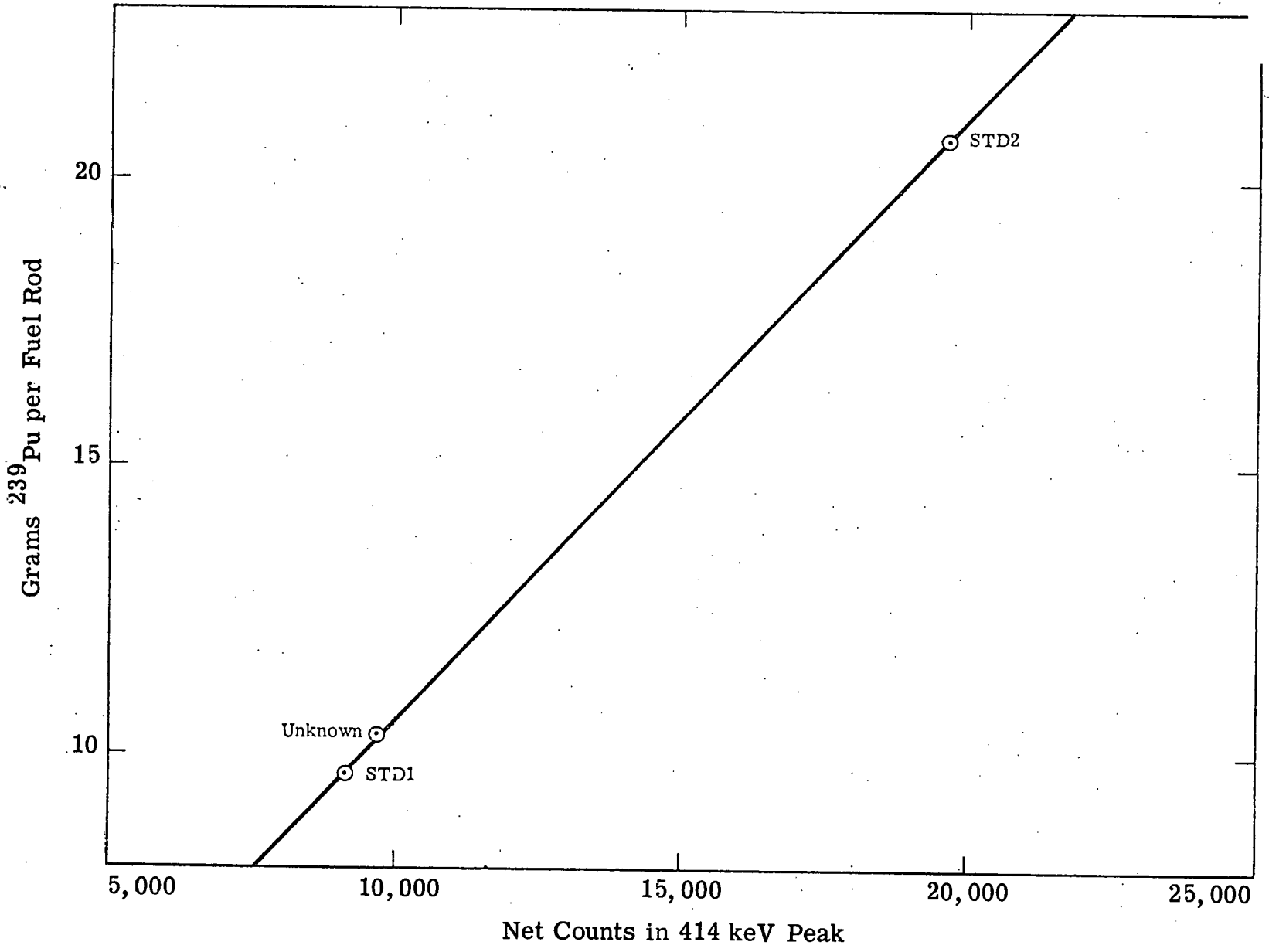

Fig. 4.8. Calibration chart for ^{239}Pu content versus net counts in the 414 keV peak.

assumptions in any assays based on standards are that (1) the contents of the standards are well known and (2) the standards are representative of the unknown samples under assay.

4.5 NaI vs. Ge(Li) Assays

We now briefly consider the problem of assaying the same ZPR fuel pins using the NaI detector setup (Fig. 4.1). The same rules and assumptions apply to the case of NaI assay as applied in the Ge(Li) assay with several important additional considerations. In the Ge(Li) assay, a single, clean peak at 414 KeV was easily identified, a simple Compton background correction made, and the net area under the peak attributed to gamma rays from the isotope ^{239}Pu.

In the case of NaI, the energy resolution is not good enough to clearly separate the strong ^{239}Pu peaks at 414 KeV and 375 KeV and a strong peak at 332 KeV with contributions from ^{239}Pu, ^{241}Am, and ^{237}U. (There are also a number of smaller peaks originating from several Pu isotopes in the same energy range.) If the (^{237}U + ^{241}Am)/^{239}Pu ratio were constant for all the fuel pins, one could conceivably relate the ^{239}Pu content to the area under the entire double-humped peak containing all three strong lines.

In the present case, however, different ZPR fuel pins contain different amounts of ^{241}Pu and hence different amounts of ^{237}U and ^{241}Am. The relative contributions of ^{239}Pu and (^{237}U + ^{241}Am) to the

double humped NaI peak are therefore different for different fuel pins. This is easily seen in Fig. 4.9 for Ge(Li) spectra of fuel pins containing different amounts of ^{241}Pu, and can also be seen with somewhat more difficulty in the case of NaI spectra taken of the same pins (Fig. 4.10). Corrections to the NaI data to separate the ^{241}Am and ^{237}U contributions from that of ^{239}Pu could conceivably be made by measuring the area under the 208 KeV peak (primarily $^{237}U + ^{241}Am$) together with the area under a collection of peaks (off-scale in the present data) in the region 650 to 750 KeV which originate primarily from ^{241}Am. There are several reports in the technical literature which describe a technique based on this approach.*

Thus, for these particular fuel pins, the poorer energy resolution of the NaI detector requires data analysis which is considerably more complicated than that described previously for the Ge(Li) system. In certain circumstances this difficulty may be sufficiently offset by the greater efficiency of the NaI which implies shorter counting times and greater sensitivity for small amounts of material. Operational constraints may also be important, such as a lack of liquid nitrogen for Ge(Li) detector cooling.

This example serves to illustrate how the basic differences in efficiency and energy resolution between Ge(Li) and NaI detectors affect the application of gamma spectroscopy to a particular assay problem. In

---

*See, for example, D. A. Bishop, E. A. Aitken, Plant Instrumentation Program Quarterly Report, GEAP-12114-3, (1970).

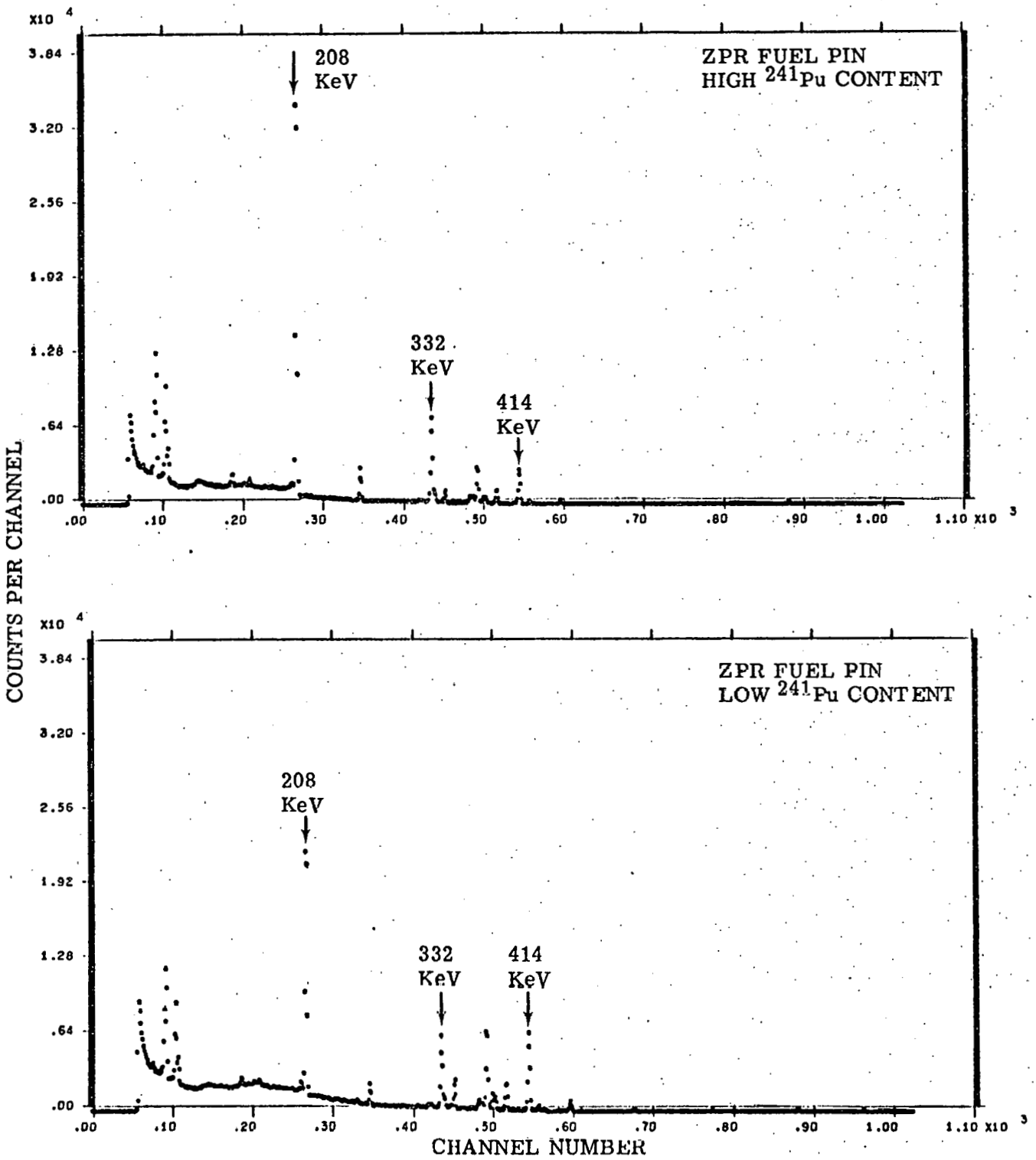

Fig. 4.9. Ge(Li) spectra of fuel pins with different ^{241}Pu content (taken under identical conditions).

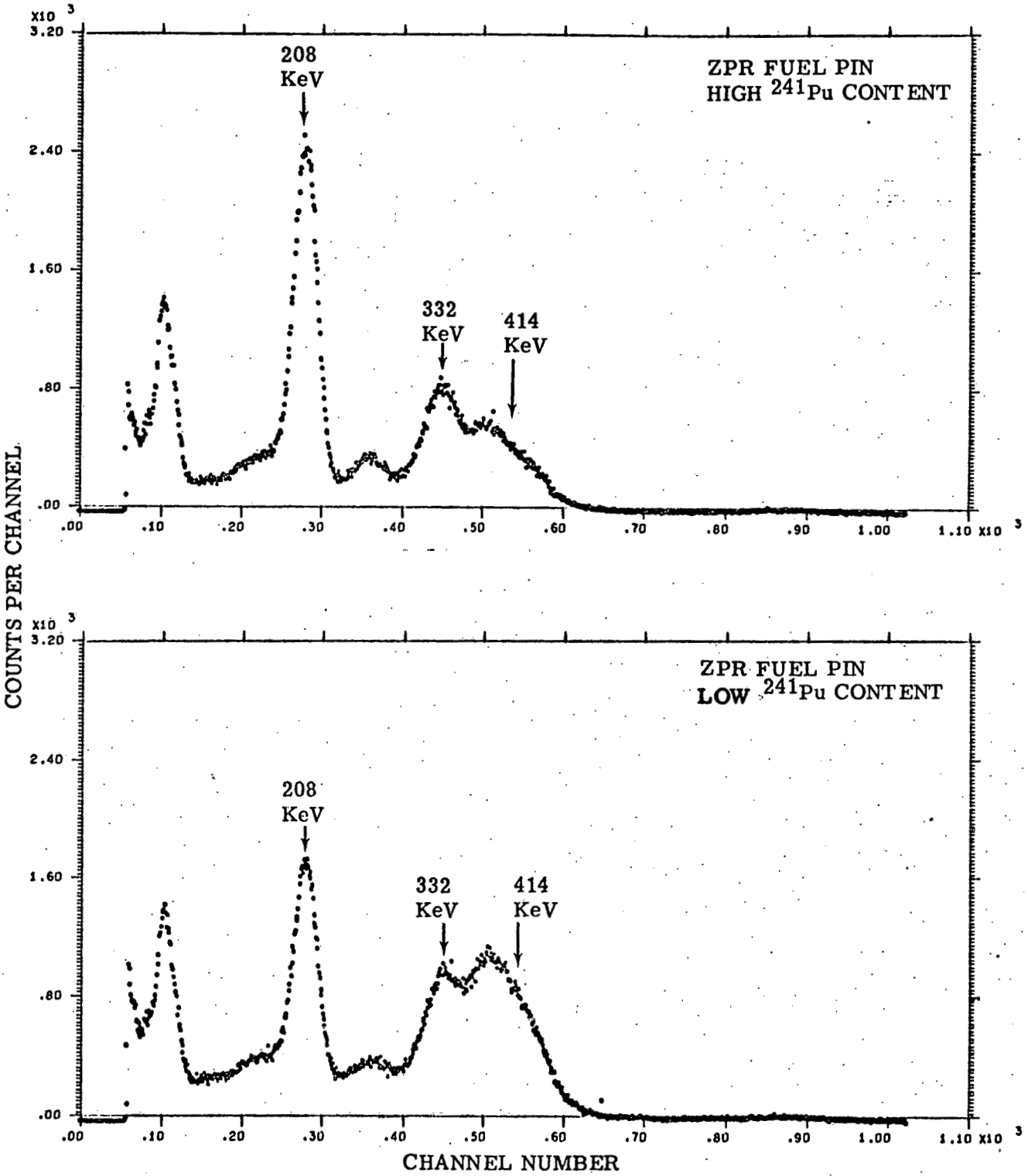

Fig. 4.10. NaI spectra of ZPR fuel pins with different ^{241}Pu content (taken under identical conditions).

general, if gamma ray spectroscopy is to be considered for a nuclear materials assay problem, the decision of whether or not to use Ge(Li) or NaI detectors depends on answers to the following questions:

1. What information is required from the assay?
2. What interferences can be expected from other materials in the sample?
3. What are the operational constraints on the system?

A working knowledge of the fundamental properties of both types of detectors is necessary in order that an intelligent choice be made. It is hoped that this document can provide an introduction to this technology and also serve as a convenient reference for some of the more basic information. As was pointed out earlier, there are many other complications which arise in the consideration of larger, inhomogeneous samples with awkward geometries and unknown content. The reader is referred to the growing collection of technical literature for further information on more difficult and challenging nuclear materials assay problems.

5. REFERENCES

The brief treatment of Ge(Li) and NaI detectors presented here is meant to serve only as an introduction to these devices for personnel involved in nuclear material Safeguards work. Additional references on gamma ray detectors which contain considerably more detail on their theory and operation are given below. Most of the introductory material presented above was obtained directly or in part from these documents. Also included below, as separate sections, are collections of references pertaining directly to the application of Ge(Li) and NaI detectors to Safeguards problems.

References for Ge(Li) Detectors (General).

1. F. S. Goulding and Yvonne Stone, "Semiconductor Radiation Detectors", Science 170 (1970) 280.

2. W. L. Brown, W. A. Higinbotham, G. L. Niller and R. L. Chase, (Eds.) Semiconductor Nuclear Particle Detectors and Circuits, National Academy of Sciences, Washington, D. C. (1969).

3. J. E. Cline, "Studies of Detection Efficiencies and Operating Characteristics of Ge(Li) Detectors", IEEE Trans. Nuc. Sci. (1968) 198.

4. J. B. Marion and F. C. Young, Nuclear Reaction Analysis - Graphs and Tables, North-Holland Publishing Co., Amsterdam.

5. D. P. Donnelly, H. W. Baer, J. J. Reidy, M. L. Wiedenbeck, "Calibration of a Ge(Li) Spectrometer for Energy and Relative Intensity Measurements", Nuc. Instr. and Methods 57 (1967) 219.

6. Proceedings: The Use of Lithium-Drifted Germanium Detectors for Research in Nuclear Physics. Vienna (1966) IAEA.

7. G. Dearnaley and D. C. Northrop, Semiconductor Counters for Nuclear Radiation - Second Edition, J. Wiley and Sons, New York (1966).

8. R. L. Heath, W. W. Black and J. E. Cline, "Designing Semiconductor Systems for Optimum Performance", Nucleonics - May (1966) 52.

NOTE: The manufacturers of Ge(Li) detectors published a large amount of useful literature concerning the operation and performance of Ge(Li) systems.

References for Ge(Li) Detectors in Safeguards Applications.

10. Proceedings: AEC Symposium on Passive Gamma-Ray Assay. November 1970.

11. J. E. Cline, "Gamma-Rays Emitted by the Fissionable Nuclides and Associated Isotopes", IN-1448 (1970).

12. J. E. Cline, E. B. Nieschmidt, A. L. Connelly, and E. L. Murri, "Technique for Assay of L-10 Bottles of Plutonium Nitrate", IN-1433 (1970).

13. R. S. Forsyth, W. H. Blackadder, "Measurements of ^{106}Ru Activity in Irradiated Fuel Elements", Proceedings: Symposium on Progress in Safeguards Techniques - Vol. I (1970) 521.

14. H. W. Kraner, "Use of Gamma-Ray Spectroscopy to Determine Pu Isotopic Abundances in Plutonium Sources", BNL 50237 (T-573) (1970).

15. P. J. Kreyger, R. J. S. Harry, H. Krockel, "Non-Destructive Burn-Up Determination by 145 keV Gamma-Ray Absorption", Proceedings: Symposium on Progress in Safeguards Techniques - Vol. I (1970) 545.

16. P. E. Rundquist, R. L. Bramblett, R. O. Ginaven, "Fission Product Gamma Rays Following Photofission for Non-destructive Assays of Fissionable Materials," Trans. ANS 13-2 (1970).

17. N. W. Beyer, T. B. Perry, R. W. Brandenburg, L. K. Hurst (Argonne National Laboratory), "Controlling Large Quantities of Plutonium Fuel", Presented at the 10th Annual INMM Meeting, Las Vegas, Nevada (1969).

18. W. A. Higinbotham, "Nuclear Safeguards", Physics Today - November (1969) 40.

19. N. C. Rasmussen, "A Review of Passive Methods", Proceedings: AEC Symposium on Safeguards R&D (1969) 96.

20. The following reports from the Gulf General Atomic (now Gulf Energy and Environmental Systems) Safeguards R&D group contain information on Ge(Li) assay systems.

GA-9077, p. 3
GA-9331, p. 12

21. The following reports from the Los Alamos Nuclear Safeguards R&D group contain information on Ge(Li) assay systems.

LA-4029-MS, p. 7
LA-4070-MS, p. 10
LA-4227-MS, p. 3, p. 8
LA-4315-MS, p. 3, p. 10
LA-4368-MS, p. 9
LA-4457-MS, p. 17
LA-4523-MS, p. 16
LA-4605-MS, p. 36

References for NaI Detectors (General).

22. K. Siegbahn (ed.) Alpha-, Beta-, and Gamma-Ray Spectroscopy, North Holland, Amsterdam (1965).

23. J. B. Birks, The Theory and Practice of Scintillation Counting, MacMillian Co., New York (1964).

24. W. J. Price, Nuclear Radiation Detection - 2nd Edition, McGraw-Hill, New York (1964).

25. A. H. Snell (ed.) Nuclear Instruments and Their Uses - Vol. I., J. Wiley and Sons, New York (1962).

NOTE: Reference 4 also contains general information on NaI detectors.

References for NaI Detectors in Safeguards Applications.

26. J. L. Lawless, R. N. Chanda, "A Plutonium Waste Counter", Trans, ANS 13-2.

27. O. H. Willoughby and D. R. Cartwright, "Measurement of Plutonium in Process Materials and Contaminated Waste", Proceedings INMM (1969) 130.

28. E. M. Sheen, et. al., "A Portable Gamma Spectrometer for Safeguards Use", BNWL 508 (1967).

29. W. Wayles, "Uranium Determination Through Gamma Counting of Production Scrap Material at General Atomic", GA-7406 (1966).

30. C. C. Webster, "A Gamma-Ray Scanner for Safeguards Use", WCAP-6030 (1959).

31. G. M. Matlock, C. F. Metz, and J. Bubernak, "Improvements in the Precise Measurement of Gamma Activity", LA-DC-7831.

32. The following reports from Gulf Energy and Environmental Systems Safeguards R&D group contain information on NaI assay systems.

Gulf-RT-10459, p. 15, p. 31.
Gulf-RT-10511, p. 32

33. The following reports from the Los Alamos Nuclear Safeguards R&D group contain information on NaI assay systems.

LA-4457, p. 19
LA-4523, p. 29
LA-4605, p. 37

NOTE: See Reference 10 for Safeguards NaI results in addition to Ge(Li) results.

34. E. K. Hyde, The Nuclear Properties of the Heavy Elements - Vol. II, Prentice-Hall, Inc., Englewood Cliffs, N. J. (1964).

35. C. M. Lederer, J. M. Hollander, and I. Perlman, Table of Isotopes, John Wiley and Sons, Inc., New York (1968).

36. Ge(Li) Handbook, Princeton Gamma-Tech, Inc., Princeton, N. J. (1969).

The above list of references is not intended to be complete, but it includes those papers which have come to the author's attention. The development of new uses and techniques for gamma-ray detectors in Safeguards applications is a growing area and the literature is extensive.

6. ACKNOWLEDGEMENTS

The following people were extremely helpful in assimilating this material and reviewing its contents.

W. Higinbotham, TSO-Brookhaven National Laboratory

M. Zucker, TSO-Brookhaven National Laboratory

E. Weinstock, TSO-Brookhaven National Laboratory

H. Kraner, Brookhaven National Laboratory

G. Llacer, Brookhaven National Laboratory

M. Kanter, Safeguards Training School - Argonne National Laboratory

R. Springer, Safeguards Training School - Argonne National Laboratory

T. Perry, Argonne National Laboratory

G. Reynolds, JRB Associates, Inc.

R. Harris, JRB Associates, Inc.